

AD-A245 616



NAVAL POSTGRADUATE SCHOOL
Monterey, California

2



THESIS

COMPOSITE STRENGTH STATISTICS
FROM
FIBER STRENGTH STATISTICS

by

Eric P. Johnson

June, 1991

Thesis Advisor:

Edward M. Wu

Approved for public release; distribution is unlimited

92-03147



Unclassified

Security Classification of this page

REPORT DOCUMENTATION PAGE

1a Report Security Classification Unclassified		1b Restrictive Markings	
2a Security Classification Authority		3 Distribution Availability of Report	
2b Declassification/Downgrading Schedule		Approved for public release; distribution is unlimited.	
4 Performing Organization Report Number(s)		5 Monitoring Organization Report Number(s)	
6a Name of Performing Organization Naval Postgraduate School	6b Office Symbol (If Applicable) AA/Wu	7a Name of Monitoring Organization Naval Postgraduate School	
6c Address (city, state, and ZIP code) Monterey, CA 93943-5000		7b Address (city, state, and ZIP code) Monterey, CA 93943-5000	
8a Name of Funding/Sponsoring Organization	8b Office Symbol (If Applicable)	9 Procurement Instrument Identification Number	
8c Address (city, state, and ZIP code)		10 Source of Funding Numbers	
		Program Element Number	Project No
		Task No	Work Unit Accession No
11 Title (Include Security Classification) Composite Strength Statistics from Fiber Strength Statistics			
12 Personal Author(s) Eric P. Johnson, LCDR, USN			
13a Type of Report Master's Thesis	13b Time Covered From To	14 Date of Report (year, month, day) June 1991	15 Page Count 112
16 Supplementary Notation The views expressed in this thesis are those of the author and do not reflect the official policy or position of the Department of Defense or the U.S. Government.			
17 Cosati Codes		18 Subject Terms (continue on reverse if necessary and identify by block number)	
Field	Group	Composite Reliability, Strand, Fiber, Statistics, Weibull Distribution	
	Subgroup		
19 Abstract (continue on reverse if necessary and identify by block number)			
Utilization of composites in critical design applications requires an extensive engineering experience data base which is generally lacking, especially for rapidly developing constituent fibers. As a supplement, an accurate reliability theory can be applied in design. This investigation is a part of a research effort to develop a probabilistic model of composite reliability capable of using data produced in small laboratory test samples to predict the behavior of large structures with respect to their actual dimensions. This work included testing of composite strength which was then used in exploring the methodology of predicting composite reliability from the parent single filament fiber strength statistics. This required testing of a coordinated set of test samples which consisted of a composite and its parent fibers. Previously collected fiber strength statistics from two different production spools were used in conjunction with the current effort. This investigation established that, for a well made composite, the Local Load Sharing Model of reliability prediction exhibited outstanding correlation with experimental data and was sufficiently sensitive to predict deficient composite strength due to a specific fiber spool with an abnormally weak lower tail. In addition, it provided an upper bound on the composite reliability. This investigation is unique in that it used a coordinated set of data with an unambiguous genesis of parent fiber and subsequent composite. The findings of this investigation are also definitive in that six orders of extrapolation of size in reliability prediction has been verified.			
20 Distribution/Availability of Abstract		21 Abstract Security Classification	
<input checked="" type="checkbox"/> unclassified/unlimited <input type="checkbox"/> same as report <input type="checkbox"/> DTIC users		Unclassified	
22a Name of Responsible Individual Edward M. Wu		22b Telephone (Include Area code) (408) 646-3459	22c Office Symbol AA/Wu

DD FORM 1473, 84 MAR

83 APR edition may be used until exhausted

security classification of this page

All other editions are obsolete

Unclassified

Approved for public release; distribution is unlimited.

Composite Strength Statistics from Fiber Strength Statistics.

by

Eric P. Johnson
Lieutenant Commander, United States Navy
B.S.M.E., University of Kansas, 1978

Submitted in partial fulfillment of the requirements
for the degree of

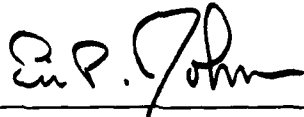
**MASTER OF SCIENCE IN AERONAUTICAL
ENGINEERING**

from the

NAVAL POSTGRADUATE SCHOOL

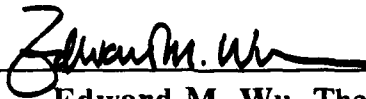
June 1991

Author:

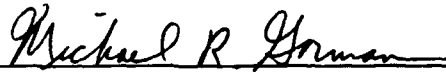


Eric P. Johnson

Approved by:



Edward M. Wu, Thesis Advisor



Michael R. Gorman, Second Reader



E.R. Wood, Chairman,
Department of Aeronautics and Astronautics

ABSTRACT

Utilization of composites in critical design applications requires an extensive engineering experience data base which is generally lacking, especially for rapidly developing constituent fibers. As a supplement, an accurate reliability theory can be applied in design. This investigation is a part of a research effort to develop a probabilistic model of composite reliability capable of using data produced in small laboratory test samples to predict the behavior of large structures with respect to their actual dimensions. This work included testing of composite strength which was then used in exploring the methodology of predicting composite reliability from the parent single filament fiber strength statistics. This required testing of a coordinated set of test samples which consisted of a composite and its parent fibers. Previously collected fiber strength statistics from two different production spools were used in conjunction with the current effort. This investigation established that, for a well made composite, the Local Load Sharing Model of reliability prediction exhibited outstanding correlation with experimental data and was sufficiently sensitive to predict deficient composite strength due to a specific fiber spool with an abnormally weak lower tail. In addition, it provided an upper bound on the composite reliability. This investigation is unique in that it used a coordinated set of data with an unambiguous genesis of parent fiber and subsequent composite. The findings of this investigation are also definitive in that six orders of extrapolation of size in reliability prediction has been verified.

TABLE OF CONTENTS

	PAGE
I. INTRODUCTION.....	1
II. BACKGROUND.....	4
A. FIBER REINFORCED COMPOSITE STRAND FAILURE MODEL.....	4
B. LOCAL LOAD SHARING.....	7
III. METHOD OF TESTS.....	10
A. DESCRIPTION OF TEST EQUIPMENT.....	10
B. TEST SPECIMENS.....	11
C. TESTING PROCEDURES.....	17
IV. RESULTS.....	20
A. TEST DATA.....	20
B. HOT-MELT ADHESIVE CONTRIBUTION TO SAMPLE STRENGTH.....	21
C. DATA ANALYSIS.....	22
D. SUMMARY.....	28
V. CONCLUSIONS AND RECOMMENDATIONS.....	32
APPENDIX A: FIGURES.....	34
APPENDIX B: TABLES.....	72
APPENDIX C: COMPLIANCE CALCULATIONS.....	83

APPENDIX D: MERGING OF STRENGTH DATA FROM
DIFFERENT SAMPLE DIMENSIONS..... 88

APPENDIX E: MAXIMUM LIKELIHOOD ESTIMATOR..... 91

LIST OF REFERENCES..... 98

INITIAL DISTRIBUTION LIST..... 100

Accession For	
NTIS GRA&I	<input checked="" type="checkbox"/>
DTIC TAB	<input type="checkbox"/>
Unannounced	<input type="checkbox"/>
Justification	
By _____	
Distribution/	
Availability Codes	
Dist	Avail and/or Special
A-1	



LIST OF TABLES

TABLE	PAGE
I. CALIBRATION DATA.....	72
II. AS4-008 2 INCH GAUGE LENGTH LOAD AND DISPLACEMENT FAILURE DATA.....	73
III. AS4-008 10 INCH GAUGE LENGTH LOAD AND DISPLACEMENT FAILURE DATA (SET B).....	75
IV. AS4-008 16 INCH GAUGE LENGTH LOAD AND DISPLACEMENT FAILURE DATA.....	76
V. AS4-008 5 INCH GAUGE LENGTH LOAD AND DISPLACEMENT FAILURE DATA.....	77
VI. AS4-019 2 INCH GAUGE LENGTH LOAD AND DISPLACEMENT FAILURE DATA.....	78
VII. AS4-019 10 INCH GAUGE LENGTH LOAD AND DISPLACEMENT FAILURE DATA.....	80
VIII. AS4-008 10 INCH GAUGE LENGTH LOAD AND DISPLACEMENT FAILURE DATA (SET A).....	81
IX. WEIBULL DISTRIBUTION PARAMETERS.....	82

LIST OF FIGURES

FIGURE	PAGE
1. Strand Failure Model.....	34
2. Composite Load Sharing Model.....	35
3. Instron Testing Instrument.....	36
4. Test Method - 2" Gauge Length.....	37
5. Test Method - 5" Gauge Length.....	38
6. Test Method - 10" Gauge Length.....	39
7. Test Method - 16" Gauge Length.....	40
8. Composite Strand Test Samples.....	41
9. Sample Test Report.....	42
10. Hot-Melt Adhesive Load Displacement Data.....	43
11. Load-Deformation Comparison of Hot-Melt Adhesive.....	44
12. MLE Probability Shift.....	45
13. 019 2" Band Width Comparison.....	46
14. 008 2" Band Width Comparison.....	47
15. 008 10" Band Width Comparison.....	48
16. 019 2" Weibull Model-Merged Composite Data Comparison.....	49

FIGURE	PAGE
17. 019 10" Weibull Model-Composite Data Comparison.....	50
18. 008 2" Weibull Model-Merged Composite Data Comparison.....	51
19. 008 10" Set A Weibull Model-Merged Composite Data Comparison.....	52
20. 008 10" Set B Weibull Model-Merged Composite Data Comparison.....	53
21. 008 10" Composite Band Width Comparison.....	54
22. 008 (All) 10" Weibull Model-Merged Composite Data Comparison.....	55
23. 019 Composite Data-Metric Relationship.....	56
24. 008 Merged Composite Data-Metric Relationship.....	57
25. 019 Composite Data (per fiber)-Metric Relationship.....	58
26. 008 Composite Data (per fiber)-Metric Relationship.....	59
27. 008-019 Composite Strength Relationship.....	60
28. 019 Fiber Data Band Width Comparison.....	61
29. 008 Fiber Data Band Width Comparison.....	62
30. 019 Weibull Model-Merged Fiber Data Comparison.....	63
31. 008 Weibull Model-Merged Fiber Data Comparison.....	64
32. 019 Fiber Data-Metric Relationship.....	65
33. 008 Fiber Data-Metric Relationship.....	66
34. 008-019 Fiber Strength Relationship.....	67

FIGURE	PAGE
35. 019 Fiber/Composite Probability of Failure.....	68
36. 008 Fiber/Composite Probability of Failure.....	69
37. 008 Composite Reliability Prediction Based on Fiber Statistics.....	70
38. 019 Composite Reliability Prediction Based on Fiber Statistics.....	71

ACKNOWLEDGEMENTS

I would like to take this opportunity to recognize those people that were instrumental in the successful completion of this work. First and foremost, my family, Travis, Kristin and most of all my wife Sherri, who's understanding, support and patience of me over the last 2 years was a much more difficult task than I had. Simply saying thank-you doesn't come close to expressing my deepest appreciation of you all. To Dr. Edward M. "MAVWICK" Wu, my mentor, who's dedication to his profession as an educator has taught me many valuable lessons that I will most certainly benefit from in all my future endeavors. It was a real honor and privilege working with you. And finally to Mr. Jim Nageotte for his assistance over the last 18 months, thanks for all your help.

I. INTRODUCTION

As more and more refinements have been developed on composite material during the past several years, the use of these materials in structural applications has become commonplace, if not the material of choice, in industry today. The reasons for this are well-known, the most common being the excellent strength-to-weight and stiffness-to-weight ratios associated with many composite materials. In addition, through micro-mechanical analysis, the engineer can design the material to optimize the physical properties (such as strength, thermal or hygro properties) for the functional requirements of the structure. As in any new developmental process, improvements to the product are always sought and the recent past has seen rapid growth in fiber improvements with respect to fiber strength characteristics. These new and improved fibers are then being used in the production of today's composite material. Associated with the rapid growth in fiber improvements is the general lack of an experience data base regarding the reliability and maintainability of the structure throughout its operational life.

The Advanced Composites Laboratory at the Naval Postgraduate School, Monterey, CA, is addressing these questions with a systematic approach to composite reliability research. Unlike traditional design and manufacturing processes utilizing materials with well known characteristics (such as aluminum) where very large design "data bases" are known which often permits "design by experience", the incorporation of composite

materials in design and manufacturing is still in its infancy, thus an equivalent "data base" does not exist. Design of a composite structure must be based on a sound reliability model of the salient physical failure process. Under tension, the failure process of a fiber composite is sequential. Internal failures start with breaking of weak fibers within the composite at relatively low applied loads. The original stresses carried by the broken fibers are transferred by the matrix binder to be shared by the neighboring unbroken fibers. This load sharing mechanism provides local redundancy thereby delaying global catastrophic failure. With the addition of external loads, more fiber failure sites are created leading to clustering of the failure sites which leads to ultimate catastrophic failure. This failure process is modeled in the Local Load Sharing model. Also, questions dealing with size effect (strength is inversely proportional to physical dimensions) of the composite structure must be addressed during the design process. This investigation is a part of the research effort to develop a probabilistic model of composite reliability which is capable of predicting actual large dimension structures from data produced in small dimension laboratory samples.

Composite reliability is a function of both the strength and life of the constituent fiber and matrix material. To establish a probabilistic model of a composite's reliability, an adequate number of experiments must be conducted which deal with the strength and life of not only the composite but also of its parent constituent fibers. The objective of this study was to gather composite strength reliability test data to be used in exploring the viability of predicting composite reliability using a Local Load Sharing

(LLS) model produced from previously obtained single fiber strength statistics. This was accomplished by testing composite strands to failure and comparing the data with the LLS reliability prediction.

II. BACKGROUND

A. FIBER REINFORCED COMPOSITE STRAND FAILURE MODEL

Graphite composite materials usually consist of high-strength, high-stiffness fiber encased in a ductile matrix. The strength characteristics of the composite are dependent on the modulus of the fiber, the modulus of the matrix and the effectiveness of the bond between the matrix and the fibers at their interface. The failure model used in this study was first introduced by B. Walter Rosen [Ref. 1]. The model addresses the failure of a composite, consisting of a matrix stiffened by uniaxial oriented fibers when subjected to a uniaxial tensile load parallel to the fiber direction. It assumes that the fibers have a statistical distribution of flaws or imperfections which results in individual fiber failures in the composite at various stress levels. The composite itself will fail when the remaining unbroken fibers, at the cross-section with the most fiber failures (weakest cross-section), are unable to carry the applied load. Therefore, in this model, the composite failure is dominated by the tensile fracture of the fibers. In analysis of the statistical distribution of flaws in an individual fiber, it has been shown [Ref. 2 and 3] that the fiber segments can be modeled as a series of links with the fiber as a chain. The chain (fiber) will fail when the applied load is large enough to cause failure of the weakest link. The statistical strength distribution of the links can therefore

be approximated by extreme value distributions which may be expressed as a two or more parameter Weibull distribution. Such distributions, when represented in a Weibull Probability of failure plot appear as linear or piecewise linear lines.

If one were to combine many individual fibers into a *bundle* and a uniaxial load was applied to it, individual fibers would begin to fail as the load on each fiber exceeded that of its weakest link. This initial failure load is much less than that of the *bundle* failure load. Once an individual fiber has failed, the load that it was carrying is now distributed over the remaining fibers within the *bundle*, increasing the applied load on each individual fiber. The broken fiber no longer carries any of the load. If the combination of the applied and the assumed load on the individual fibers remaining is less than its weakest link strength, then the fiber will remain intact. If it is greater, then the fiber will fail and the same transfer of loading takes place. This process will continue as the applied load is increased and *bundle* failure will occur once every individual fiber has been broken.

When the fiber bundle is encased in a matrix, the failure process of the newly formed *strand* is changed from that of the *bundle*. The model that describes the *strand* failure consists of parallel fibers in an otherwise homogeneous matrix. Its fiber statistical strength distribution is assumed to be the same as before. Figure 1, Appendix A shows the failure model presented by Rosen [Ref.1]. It should be noted that in this model, the extensional stresses in the matrix are neglected relative to those in the fiber and the shear strains in the fiber are neglected relative to those in the

matrix. This is a reasonable assumption for fibers that are very strong and stiff relative to the matrix. As a uniaxial load is applied to the *strand*, the fibers with the weakest links begin to fail just as described in the *bundle*, but unlike the *bundle*, the matrix provides a unique load sharing characteristic that enables the internal broken fiber to continue carrying an applied load. In the vicinity of an internal failure, the uniaxial load that was carried by the fiber is transmitted by shear through the matrix to adjacent fibers. These adjacent fibers now carry a load increased by a load concentration factor (K_f). The internal failures result in shear stresses that locally may attain very high values. At the fiber end (point of failure), stress (σ) goes to zero and the shear (τ) goes to a maximum value. Therefore, a portion of the fiber near the fiber end is *ineffective* in resisting the applied load. This distance is known as the *ineffective length* (δ). Rosen has shown [Ref. 1] that the ineffective length (normalized to the fiber diameter) of this model to be

$$\frac{\delta}{\delta_f} = \frac{1}{2} \left[\left(\frac{1 - \nu_f^{1/2}}{\nu_f^{1/2}} \right) \left(\frac{E_f}{G_m} \right) \right]^{1/2} \cosh^{-1} \left[\frac{1 + (1 - \phi^2)}{2(1 - \phi)} \right]$$

- where
- δ_f is the fiber diameter
 - ν_f is the volume fraction of fiber in the composite
 - E_f is the modulus of the fiber
 - G_m is the shear modulus of the matrix
 - ϕ is the fraction of the undisturbed stress value below which the fibers shall be considered ineffective

As the applied load increases, the number of statistically distributed fiber failures increase, producing an accumulation of ineffective fiber lengths. When a sufficient number of these ineffective fiber lengths combine in the vicinity of one cross-sectional area of the *strand*, it results in a weak surface. This enables the onset of matrix/fiber interface debonding and/or crack propagation through the matrix, ultimately resulting in the composite failure. In summary, the models treat fiber failures as the result of a statistically distributed flaw (weakest link). Composite strand failures are the result of a statistical accumulation of the fiber failures over a given cross-sectional area. Therefore, fiber strength is dependent on length; that is, longer chains (fibers) have a higher probability of having a weaker link (flaw) than a shorter chain. This agrees with experimental data [Ref. 4] that demonstrates that fiber strength is a monotonically decreasing function of fiber length.

B. LOCAL LOAD SHARING

The Local Load Sharing model used in this study was developed by D. G. Harlow and S. L. Phoenix [Ref. 2 and 3] and is shown in Figure 2, Appendix A. The fiber-matrix composite is viewed as a planar structure of n parallel fibers partitioned into a series of m sections, called bundles, each with n fibers. Conceptually, each bundle (defined as the metric) can be any desired length. Harlow and Phoenix designated the metric length to be the ineffective length δ . The length of the material is then simply the metric length times m . In the model, the bundles are considered to be statistically independent and the strength of the composite material is that of its weakest

bundle. In addition, it is assumed that the strength of the fiber elements are statistically distributed and can be modeled by the Weibull distribution

$$F(L) = 1 - \text{EXP} \left\{ - \left(\frac{L}{\beta} \right)^\alpha \right\} \quad \text{for } L \geq 0$$

where α is the shape (slope) parameter

β is the location parameter

L is the independent variable

As shown in Figure 2, Appendix A, if the bundle load is x (per fiber) then the adjacent surviving fiber elements carry a new load $K_r x$ where

$$K_r = 1 + r/2 \quad r = 1, 2, 3, \dots$$

and r is defined as the number of consecutive failed fiber elements immediately adjacent to the surviving element (on both sides). K_r is called the load concentration factor. The probability distribution of the strength of a composite with Weibull distributed parent fibers can be computed numerically using a recursive relation for different fiber failure cluster (K_r) configuration. Based on this exact calculation, an approximate representation is available [Ref. 5] and is summarized as follows:

$$H_{mn}(L) \cong 1 - \{1 - W(L)\}^{mn} \quad \text{for } L \geq 0$$

where $W(L) = \min F^{(k)}(L)$ for $L \geq 0$ and $k = 1, 2, 3, \dots$

and $F^{(k)}(L) = 1 - \text{EXP} \left\{ - d_k \left(\frac{L}{\beta} \right)^{k\alpha} \right\}$ for $L \geq 0$

$$d_k = d_k(\alpha) = 2^{(k-1)} (K_1 K_2 K_3 \dots K_{k-1})^\alpha$$

$$K_r = 1+r/2 \quad \text{where } r = 1,2,3,\dots$$

with the variables $H_{mn}(L) \equiv$ Probability of failure of a composite of length m times the metric length

$W(L) \equiv$ Probability of k - failure in the bundle

$F(L) \equiv$ Probability of failure of the mn fiber elements

$k \equiv$ The number of adjacent fiber breaks in a bundle

$d_k \equiv$ A constant that is a function of α

and K_r , r , α , β and L are as previously defined. Finally, it is important to note that for a poorly made composite with inferior fiber/matrix adhesion and voids, the failure process will approach that of the global load sharing of a bundle rather than the local load sharing of a composite.

III. METHOD OF TESTS

A. DESCRIPTION OF TEST EQUIPMENT

1. Mechanical System

The strand tensile strength testing was conducted utilizing an Instron Universal Testing Instrument, model 4206, shown in Figure 3, Appendix A. It is comprised of two major systems: a crosshead drive and control system, which applies tensile or compressive loading to a specimen; and a highly sensitive load weighing system, which measures the load applied to a specimen.

An Instron 2512 series, 1000 Kilogram load cell which was used to measure applied loads, was mounted in the moving crosshead which is operated by two vertical leadscrews within the loading frame.

The test articles (composite strand samples physically resembling a pencil lead) were held by two Instron Modular Hydraulic Wedge Collet Grips (series 2742), one mounted on the load cell and the other on the base of the machine. One-half inch diameter collets were used in the wedge grips for mounting the specimen into the grip. The specimens were held stationary in the grips by hydraulic pressure obtained by a Instron Electric Pump Pressurization System (model A7154, Rev D, #5215) shown in Figure 3, Appendix A. The unit is self-contained with gripping pressure fully adjustable and independent of system pressure or fluctuations such that gripping force remains constant on the sample under test.

2. Control and Data Acquisition System

The control and data acquisition of the testing instrument was automated with the use of Instron Series IX Materials Testing System. This system is a software package that interfaces the test instrument with a personal computer. The testing system components included the Series IX software, an IBM/PC-AT computer (1.5 MB of RAM, 30 MB hard disk) with an EGA monitor, an IEEE-488 (GPIB) interface, an IBM Proprinter II parallel printer and an HP 7470A plotter for graphic functions.

The software, which is menu driven, presents the operator several options including computer controlled testing, reanalysis of data, calibration of the test instrument, creating and or modifying the test method to be used in the computer controlled testing, and plotting of the raw data. Separate test methods were created for each gauge length of samples tested and are presented in Figures 4, 5, 6 and 7, Appendix A.

B. TEST SPECIMENS

1. Sample Composition

The test specimens were produced from a Hercules Magnamite high strength graphite, type AS-4. Both the fiber samples and the composite samples were fabricated from two specific production spools designated as 008 and 019. Each composite strand consisted of 3000 fibers with a nominal cross-sectional area of $.66 \text{ mm}^2$. Samples with different gauge lengths were tested, the majority of which were 2 and 10 inches for spool 008 samples, and 2 inches for 019 spool samples. Ten inch samples from the 019 spool were tested in previous investigations and are also included

for interpretation.. Two additional samples, one 5 inch and one 16 inch gauge length were also tested and this data used for compliance calculations in addition to normal data reduction.

2. Test Method Development

The samples were required to be made such that the strand could be gripped and held under load in the testing instrument. In addition, it was desired that the strand fail in the gauge length area and not in the gripping area. Two different testing methods were identified and investigated to accomplish these requirements. The first method involved securing the test strand ends in a copper tube (.0669 inch OD and .0390 inch ID) utilizing an epoxy type adhesive with the tubes separated by the desired gauge length. The two ends were then be placed in an adapter collet (from a manufactured jeweler's lath having .0700 inch ID and .500 inch OD) which in turn were placed in the grips of the testing instrument. Several problems were encounter in the implementation of this method. First, the adapter collet/copper tube interface area was too small, producing a high stress concentration area on the strand itself upon gripping, causing failure of the strand in the grip. Also, the adapter collets were not designed to accept the type of loading the gripping procedure produced and they failed after a relatively low number of loadings. The second method involved using one-half inch aluminum bar stock to make 1/2 inch long pellets that were secured to the ends of the strands with the epoxy, resulting in a "dumbbell" type configuration of the test strand. Each pellet had a #60 drill size hole (dimensions) machined into the center of it to accommodate the ends of the strands. This configuration allowed the test samples to be

placed directly into the testing instrument, thereby simplifying the test procedures. Jigs, which were made out of aluminum angle iron, were designed and manufactured to maintain the pellets at the proper gauge length during the adhesive bounding process. At the same time, the jigs protected the samples from handling damage. This was the procedure that was followed to make the test articles and is explained in further detail in the following sections.

Application of hydrostatic pressure, via the hydraulic grips, to the pellets produced a hydrostatic state of compressive stress in the sample/aluminum pellet interface. This increased the shear strength of that portion of the strand which facilitated the transfer of the external load to the fiber filaments within the free strand. Through trial and error, it was determined that a reduction of .0025 to .0035 inches of the outer diameter of the aluminum pellet upon application of gripping pressure was sufficient to produce an effective hydrostatic pressure. This amount of deformation was also the limit to prevent permanent deformation of the collets inside the grips themselves. To consistently obtain the desired yield characteristics, the pellets were all annealed at 450 deg Celsius for 1 1/2 hours and then oven cooled overnight. This not only produced the desired deformation properties but also acted to rid the pellets of any residual oil and dirt deposited during the machining process. The annealed pellets were then tested by applying incremental steps of hydraulic pressure to the grips holding the pellet to determine the gauge pressure in the testing system that produced the desired deformation. This optimal pressure was estimated to be 500 psi indicated.

3. Stress Wave Attenuation

The intended purpose of a stress wave attenuator was to prevent secondary failures of the strand sample caused by the stress wave accompanied by the initial failure. Immediately after the initial failure of the sample the tensile energy stored in the unbroken portion of the sample is released resulting in a tensile stress wave traveling toward the two ends of the grip. Upon reflection from the strand/pellet grip interface, the tensile wave is converted to a compressive wave. Since the strand sample is long and slender, the compressive wave almost always caused a secondary failure at the strand/pellet interface due to compress buckling. Additional secondary failure sites throughout the length of the sample were also frequently observed, thereby precluded a definitive identification of the original initial failure site. It was experimentally observed that when the tensile stress was attenuated during the initial propagation stage, the secondary breakages could be eliminated. Because in the current testing configuration, the test sample was gripped in a vertical position, sand and oil were ruled out as candidates as stress wave attenuators, even though both of these have proven successful in the past.¹ The use of paraffin wax was also attempted but without success, as was modeling clay. The material adopted for these tests was a commercially available generic hot-melt adhesive that was applied, via a hot melt glue gun, to the entire gauge length of the test specimen. The general chemical constituents of the

¹ Wu/Nypiuk testing at Livermore Lab

adhesive include a styrene derivative, a hydrocarbon resin, artificial wax, and ethylene vinyl acetate copolymer resins.

4. Test Specimen Preparation

The composite strands were originally manufactured in approximately 18 inch sections and cut to lengths that were 1 1/4 inches longer than the desired gauge length by the use of a Dremel tool (using a cutoff grinding wheel attachment). The additional length was used to insure the strand extended through the entire length of the pellet. Once the required number of samples were cut (8 samples per batch), each end was cleaned by rinsing them through two separate acetone baths using a glass syringe. Additionally, the utensils (stirring stick and the syringe used for the placement of the epoxy) were also cleaned in the same manner. An epoxy that consisted of 55% by weight Dow DER-332 Epoxy Resin and 45% by weight Texaco Jeffamine T403 was then made and stirred for a minimum of 3 minutes to ensure thorough mixing. The epoxy was then placed into a vacuum chamber to rid it of the air bubbles developed while mixing. This epoxy was used because of its particularly good wetting properties and its slow setting time. This allowed sample preparation to be conducted in a slow, methodical process reducing the possibility of damaging the samples during manufacturing.

The pellets that were attached to the end of the strands (2 each) were then prepared by placing cellophane tape on three of the four ends of each set of pellets with small holes punctured through the tape in the center of each machined hole in the pellet. The use of a pin and microscope helped in placing the puncture hole in the desired location. This process

was done to help center the strand in the pellet during the production of the test samples. The pellets were then placed in the jigs with the pellet with tape on both sides being the bottom pellet and the top pellet having the taped side down. They were held in proper place in the jig by rubber bands, allowing for the easy removal (cutting of the rubber bands) of the test sample from the jig at time of testing. The rear portion of the angle iron type jigs was machined away enabling access to the rear of the strand, making the application of the hot-melt adhesive easier. Once the jigs and the strands were prepared and ready, the epoxy was placed into a plastic, reusable syringe with a modified tip consisting of the bottom tip of a 5 mm mechanical pencil. This modification allowed the injection of epoxy directly into the top holes of the pellets until the epoxy flowed out the bottom. Since test samples were made in batches of eight, each of the 16 pellets were filled with epoxy in this manner. The strands were then inserted into the pellets such that the strand extended through the entire length of each pellet. The jig was then placed in a vertical stand. Surface tension retaining the liquid epoxy in the cavity of the pellet alleviated the problem of inadvertently attaching the pellet to the jig. Once all eight samples were made, the stand was placed in an oven which was pre-heated to 58 deg Celsius (to accelerate cross-linking of the epoxy) and cured for 24 hours. After curing of the adhesive in the pellet, each sample had the hot-melt adhesive applied, by hand, to the entire length of the strand. The samples were then ready for testing. Figure 8, Appendix A shows the completed samples.

C. TESTING PROCEDURES

1. Alignment

Before any testing was conducted, the test instrument's upper and lower grips were aligned by gripping a precision ground 1/2 inch diameter steel drill rod in the grips with the grip surfaces separated by approximately 1/4 inch. A load of 1000 Kg (the load cell design limit) was then carefully applied and maintained (ensuring the load never exceeded design limits). To eliminate all of the mechanical play or looseness in the system, all of the rigid coupling attachments were then tightened under this tension, thereby setting the alignment of the grips. To ensure a consistent mechanical reference state for every sample tested, the grip alignment was checked and verified approximately one-half way through each testing interval.

2. Calibration

Load cell calibration was conducted before, during and after the testing period. Calibration was conducted using Instron calibration weights (traceable to National Bureau of Standards) with load increments of 5 Kg. Calibration data is presented in Table I, Appendix B. In addition, a time drift or stability check of the system was conducted over a 24 hour period utilizing a constant load of 15 Kg. The greatest drift recorded during the period was within .17 per cent of the original load. As shown, the calibration remained well within the published specification limit of $\pm 1.0\%$.

3. Testing

Testing of the prepared samples involved transferring the samples from the jigs to the test instrument and initializing and starting the test via the computer. The fully automated testing system recorded all the data and stopped the test upon failure of the sample.

The placement of the sample into the test instrument required two people, one to assist the pellet of the strand in sliding into the collets internal to the grips and the other to operate the console that controls the crosshead displacement. The sample was first placed into the upper grip and inserted far enough into the collet such that the lip of the pellet was inserted beyond the lip of the collet. This ensured that the gripping force was distributed over the entire surface area of the pellet. A gripping force, measured by a hydraulic gauge pressure, of approximately 500 psi was then applied to the grip housing via the hydraulic pump. The crosshead was next lowered (manual mode, fast speed) such that the bottom pellet was approximately 1/4 inch above the upper surface of the lower grip housing. At this point, the speed select was changed to manual mode, slow speed and a load balance was conducted. Then the bottom pellet was inserted into the collet of the lower grip to the same relative position as previously described and gripping pressure applied. The crosshead was adjusted such that a slight negative load (0.0 to -10 Kg) was indicated. The crosshead position reference was then reset to zero completing the installation.

The computer was initialized, dependent on gauge length, utilizing the appropriate test method program. Sample identification numbers were developed such that they could be easily identified. For example, sample

01902-15 was the 15th sample of 2 inch gauge length of the AS4-019 class of composite strand that was tested. Once the required information of the interactive program was entered, the test was conducted. After testing to failure, the sample was removed from the test instrument and examined to determine the location of failure. A summary of all pertinent data collected during each test was then documented in the computer generated test report. A sample test report is presented in Figure 9, Appendix A. The raw data was finally stored on the hard disk and backed up on a floppy disk.

IV. RESULTS

A. TEST DATA

1. Current Testing

A total of 82 strands were tested to failure of which 56 were from the AS4-008 graphite spool and 26 from the AS4-019 spool. Load and displacement at failure data for all tests are presented in Tables II thru VI, Appendix B. Compliance calculation methodology for the correction factor applied to sample displacements due to system mechanical displacement is discussed in Appendix C.

2. Previous Testing

Data from previous tests of 008 and 019 composite strands that were part of the same physical set of the current test samples has been included in the data base for use in the analysis of data in this report. This was done to better define the reliability curve that the process of data reduction produces. The source of this data is from tests conducted at Lawrence Livermore National Laboratories by Dr. Edward M. Wu and Mr. Glenn Nypiuk [Ref. 6]. This data is presented in Tables VII and VIII, Appendix B. AS4-008 data from these tests are designated set A as compared to AS4-008 data set B which designates current test data.

Fiber strength research for both (008 and 019) graphite spools was conducted by Dr. Edward M. Wu and Mr. Nypiuk [Ref. 6], Lt. David Keith Bell, USN [Ref. 7], LCDR Carl Engelbert, USN [Ref. 8] and Mr. Jim Nageotte of the Advanced Composites Laboratory, Naval Postgraduate

School. The fiber data from the above research, which is to be used in the final analysis of the present research, is contained in Ref. 9.

B. HOT-MELT ADHESIVE CONTRIBUTION TO SAMPLE STRENGTH

By using hot-melt adhesive as a stress wave attenuator, the question arises that, what contribution, if any, does the hot-melt adhesive make to the strength of the sample? This issue was resolved by testing the adhesive and determining its modulus which was then compared to that of the strand. Graphical representation of the hot-melt load-displacement data is presented in Figure 10, Appendix A. Knowing the cross-sectional area of the test sample, the modulus of the adhesive was calculated to be $2.845E3$ lbs / in². When compared to the modulus (approximated at $20E6$ lbs / in²) of the composite strand, this is less than .014 per cent of the strand modulus. In addition to the modulus comparison, experiments were conducted to determine the effect the addition of the adhesive to the strand would make on the raw data. This was done by first testing a single strand (without adhesive) to a load of approximately 50% of the failure load. This load application procedure was repeated several times to ensure that all the fibers that were weak and would break under a load up to and including the peak applied load, actually broke. This resulted in a fixed, repeatable, load-displacement curve for the test sample, indiscriminate of how many times a load (of the same peak magnitude) was applied. The hot-melt adhesive was then applied to the strand and the sample tested to the same load as before. As can be seen in Figure 11, Appendix A, the

load-deformation curve of the sample with the adhesive lies directly on top of the same curve of the sample without the adhesive.

In analyzing the results of both of these experiments, it was concluded that in the context of the testing done to the composite strands on this project, that the hot-melt adhesive *did not* add to the strength of the composite strand and therefore the use of the hot-melt adhesive as a stress wave deflector *did not* effect the data.

C. DATA ANALYSIS

1. Data With Experimental Artifact

In this type of data analysis, the data of those strands that failed in the gauge length portion of a test sample are considered the *intrinsic* load of that particular sample. The question then arises of how should the data of the samples that have multiple failure sites including one failure site at the grip/strand interface, be handled? We classified this data as censored data (due to the potential experimental artifacts which may have lowered the strength). Based on this physical consideration, the failure load (\hat{L}_i) for censored data samples must be always less than and at best equal to its intrinsic value, that is, (L_i) or $(\hat{L}_i) \leq (L_i)$. Our goal is to be able to use this censored data in combination with the intrinsic data in the data analysis. To achieve this, during data analysis a procedure using the Maximum Likelihood Estimator (MLE) was utilized. The MLE concept for a two parameter Weibull distribution is discussed in Appendix E.

In data analysis, it is desired to plot the Weibull probability of failure of the material $F^*(L_i)$ versus its intrinsic load. To do this, one must *order* the experimental data (failure load) in ascending order and

assign a *rank* to each point. In this analysis, expected ranking was used such that the rank of (L_i) is

$$\frac{x}{N+1} \quad \text{for } x = 1, 2, 3, \dots, N$$

where x is the numerical sequence of the failure load after ordering and N is the total number of samples tested. Because some of the data is censored and not intrinsic, a MLE analysis is conducted to estimate the model of, or the parameters of, the Weibull distribution associated with this particular set of data. A new probability of failure $\bar{F}(\hat{L}_i)$ is then determined for each point of censored data (\hat{L}_i) as shown in Figure 12, Appendix A. In analyzing $\bar{F}(\hat{L}_i)$, we note that if $\bar{F}(\hat{L}_i) > F(\hat{L}_i)$, it physically implies that the failure load (\hat{L}_i) was greater than its intrinsic load (L_i) or $(\hat{L}_i) > (L_i)$, which is inadmissible in the physical model. Therefore, in this case, for each point where $\bar{F}(\hat{L}_i) > F(\hat{L}_i)$, we assume $(\hat{L}_i) = (L_i)$ and $\bar{F}(\hat{L}_i) = F(L_i)$ or that the failure load is the intrinsic load. If $\bar{F}(\hat{L}_i) < F(\hat{L}_i)$, the value of $\bar{F}(\hat{L}_i)$ is carried forward in the calculations. The new values of $\bar{F}(\hat{L}_i)$ are then combined with the original ranking of the intrinsic loads and the rank (with rank remaining keyed to the load) is reordered in ascending order. It should be noted that the MLE process should be performed on a sample set of a single dimension only. This is based on the fact that when the range of the probability of failure, $F(L_i)$ {ie, the sample size N } is small, the assumption of a linear Weibull distribution is a good approximation of the model. In other words, the model is assumed to be piecewise linear when the sample size is small.

2. Data Considered Intrinsic

This type of analysis assumes that the failure load of a particular test sample is the *intrinsic* load of the sample, or the sample failed at its statistically distributed intrinsic stress level or load. This assumption excludes any experimental artifact that may be associated with the data. This is the basis of the analysis used in this investigation.

a. Data Interpretation

Since both composite and fiber strength are functions of gauge length, a mathematical model must be determined to normalize all the data to one single metric size so that a direct comparison of all the data can be made. The standardization by a metric dimension can be chosen arbitrarily without affecting the relative relations. The metric selected by the current data analysis is one centimeter. The method for this standardization to a common metric dimension is discussed in Appendix D. The standardization used in the data analysis of this study is the vertical shift type.

To determine if the data of like materials and gauge lengths are of the same set (identical test samples), the Weibull probability of failure plots are compared for each batch of tests completed. Figures 13, 14, and 15, Appendix A show a comparison of each batch of data collected. In the analysis, batch one was the first half of the sample set which was compared to the second half of the sample set. Batch two compared all the odd number test samples to that of the even number test samples. The data band width is dependent on the experimental circumstances. A narrow band implies that the experimental techniques among the batches are

similar, justifying the merging of the different test batches into one data set. As shown, the data band width for each of the sample sets is narrow, indicating that the data belongs to the same set, which is consistent to the actual experimental circumstances. By confirming that like batches are the same, they can be merged to produce single sample sets of like materials and gauge lengths. Figures 16 through 20, Appendix A presents the merged data of the sample sets as compared with the assumed Weibull distribution model obtained with the use of a Maximum Likelihood Estimator as described in Appendix E. The band width of the two sets of 008 10" data (sets A and B) was then analyzed as shown in Figure 21, Appendix A and the two sets determined to be of the same set. The 008 10" data was then merged and compared to the assumed Weibull distribution model as shown in Figure 22, Appendix A. The values of α and β produced by the MLE method for each set of data are presented in Table IX, Appendix B. All the data was then converted to a 1 cm metric format to enable a direct comparison with fiber data of the same metric. Figures 23 and 24, Appendix A present this data in terms of composite sample strength (per bundle) and Figures 25 and 26, Appendix A present it in terms of composite strength per fiber in a bundle. As shown in Figure 27, Appendix A, in a direct comparison of composite strength (per fiber), the composite made with the 008 spool of AS4 fiber appears to be stronger than that made with the 019 spool of fiber even though both spools came from the same manufacturing line and were assumed to be identically produced. This is an indication that fiber spools that may have even been

produced in the same line, let alone the same lot, have to be regarded as having different statistical characteristics and treated as such.

Much the same type of analysis can be done with the fiber data. Figures 28 and 29, Appendix A show the band width of the fiber data, which confirms that the data belong to the same set of like materials and gauge lengths. Figures 30 and 31, Appendix A present the merged fiber data as compared with the assumed Weibull distribution model. The values of the trimodal Weibull distribution for this data are presented in Table IX, Appendix B. As noted in Figure 30, Appendix A, the 019 fiber probability of failure is judged to be bimodal, or the lower tail having different Weibull distribution parameters than the upper tail. The modal shape of the data was determined by visual examination of merged individual ordered data plotted on a Weibull axis. The data was then identified, in this case, as either unimodal or bimodal. The fitting of the data to the upper and lower curves, including the identification of the lower transition point was performed heuristically. The MLE program was used to determine the values of α and β for both the lower and upper curves. The use of MLE is permitted for the bimodal case because it is considered to be a piecewise linear distribution in the Weibull plot with a distinct transition point. Figures 32 and 33, Appendix A present the Weibull probability of failure of the fiber when converted to a metric of 1 cm. Figure 34, Appendix A shows the comparison of the fiber strengths and is consistent with Figure 27, Appendix A.

b. Local Load Sharing Analysis

The data from Figures 25 and 32, Appendix A were combined to produce Figure 35, Appendix A. Likewise, Figures 26 and 33 were combined to produce Figure 36, Appendix A. These plots are used in conjunction with the Local Load Sharing (LLS) Prediction Model with extensions, to enable prediction of composite reliability from trimodal Weibull fiber statistics [Ref. 10]. The model requires two inputs, the fiber model parameters and the *ineffective* length, in order to predict the model for the composite reliability. The *ineffective* length, however, is not known, so the LLS program [Ref. 10] was written in a normalized (X_i/β) format. Therefore, when the model parameters of a particular set of fiber data are used in the program, the LLS curve that is produced is referenced to the normalized composite data of the same gauge length. In this analysis, one set of data (ie, the 008 data) was used in the model, since both the fiber and composite statistics (Figure 36, Appendix A) were known. Fiber statistics were entered using the model parameters in a trimodal Weibull distribution format. The model then generates a predicted value for the composite reliability from which the *ineffective* length is estimated. This is done by shifting the predicted reliability model horizontally to the right until the model approaches the value of the associated composite test data. Since the amount shifted is a function of the *ineffective* length of the composite, it is assumed to be the same for a composite made of the same fiber (AS4) but of different spools. The same magnitude of shift is then used in conjunction with the 019 fiber statistics and the LLS model to predict the 019 composite reliability. This prediction can be compared and

cross-plotted directly with Figure 35, Appendix A, making analysis of the LLS Prediction Model possible. The process can also be reversed by using the 008 data to obtain for the *ineffective* length and then predicting the 019 composite reliability with the LLS model, which can then be compared with Figure 35, Appendix A. Figures 37 and 38, Appendix A presents the graphical comparison of the predicted composite reliability and the experimental test data for both 008 and 019 sample sets.

As can be seen in Figures 37 and 38, the LLS composite reliability prediction exhibits outstanding correlation with the experimental data. In addition, it is sufficiently sensitive to predict the shifted composite strength due to the abnormally weak fiber tail associated with the 019 fiber. It can also be inferred that the LLS reliability prediction provides the upper bound on reliability since the model assumes a well-made composite with a consistent ineffective length. This is further supported by the fact that the experimental data of the test specimens (which are considered well-made) correlated so closely with the predicted model.

D. SUMMARY

In summary, the major effort of this investigation was in the collection of a comprehensive set of composite data to be interpreted in conjunction with parent fiber data sets previously collected. The model for the data interpretation is the Local Load Sharing model which uses fiber statistics to predict the spatial density and clustering of the fiber failure sites. From the local stress concentrations that arise from load sharing, the probability of composite failure is predicted. This analytical prediction is then compared to the composite strength data sets obtained in this investigation.

Since the constituent fiber statistics are the benchmark for composite reliability prediction using the LLS prediction model, it is important to ensure that the experimental fiber data was obtained in such a manner that the data accurately reflects the statistical distribution of the fiber strength. This was accomplished in previous investigations by testing a sufficiently large sample population which ensures that the modal occurrence and the trimodal Weibull distribution parameters estimated are representative of the underlying fiber population. In addition, the use of multiple operators in conducting the tests also prevented the inadvertent skewing of the data. Finally different spools of fiber were used to identify normal manufacturing variables that are always present during the production process.

To verify the prediction model with composite test data, the composite data must again be beyond question in proper representation of composite strength statistics. In this investigation, much time was spent in developing the test method procedures to ensure that the experimental data was accurate. The test sample gripping technique developed and utilized for the longitudinal tension testing was designed to prevent the normally dominant shear failure mode associated with tension testing from causing the test specimen failure. This was accomplished with a unique encapsulating grip that applied hydrostatic pressure to the sample at the grip/sample interface which was induced by static compression. The use of the hot-melt adhesive to attenuate the stress wave that accompanies the sample failure, prevented the shattering of the sample and enabled the identification of the failure characteristics. In addition, different sample dimensions (gauge lengths)

were tested to extend the data range and enable the use of the methodology of data interpretation by shifting the weakest link. All this was successfully accomplished, producing great assurance in the experimental results.

In interpretation of the data, for the case where the fiber is unimodal, the parameters for the two parameter Weibull distribution were estimated using the maximum likelihood estimator. For the case of data (019 spool of fiber) which displayed a bimodal distribution a model consisting of three piecewise linear Weibull distributions was used. The parameters for the trimodal Weibull distribution model were estimated from the ordered data set with censoring to the left and right respectively. The composite test samples that were used in this investigation were considered to be exceedingly well-made composite strands with uniform fiber and matrix adhesion and therefore, a uniform ineffective length. The ineffective length is controlled by the interfacial strength (a function of the manufacturing process) and the shear modulus of the matrix (materials). Composites with irregular fiber-matrix adhesion and voids have large ineffective lengths, the limiting case being a composite with no matrix (a bundle). It was observed that for this set of well-made composite, the Local Load Sharing Model of reliability prediction exhibited outstanding correlation with experimental data and was sufficiently sensitive to predict deficient composite strength due to a specific fiber spool with an abnormally weak lower tail. In addition, it provided an upper bound on the composite reliability. The documented weaker lower tail of the 019 fiber was predicted in the composite reliability by the LLS model, verifying six orders of extrapolation of size in reliability prediction. It

should be noted that all analytical results were consistent with experimental observation, not only in trend but also in substantial agreement with magnitudes.

V. CONCLUSIONS AND RECOMMENDATIONS

The results of this investigation suggest that the Local Load Sharing composite reliability prediction method using a trimodal Weibull distribution is a viable method of predicting composite structural reliability using fiber strength statistics. In design, this methodology provides a relation of strength data, based on small laboratory sample dimensions, to actual large structural dimensions for a fail safe design. In materials development, this methodology can be used to identify the parametric role of fiber and matrix strength properties for possible improvements. In manufacturing, this methodology can be used to prescreen fiber for zero-reject fabrications. In maintenance and repair, this methodology provides quantitative guidelines.

The following areas were not fully treated in this investigation and are recommendations of follow-on research:

1. That larger physical dimension test samples be tested such that next several orders of data extrapolation can be verified.
2. That a mathematical formalism of the statistical methods to estimate the parameters for the trimodal Weibull distribution be established.
3. That a mathematical formalism of the statistical methods to estimate the best fit ineffective length based on the composite and fiber data be conducted.

4. That a closed form approximation of the Local Load Sharing composite reliability prediction method using trimodal Weibull distribution parameters be developed.

APPENDIX A

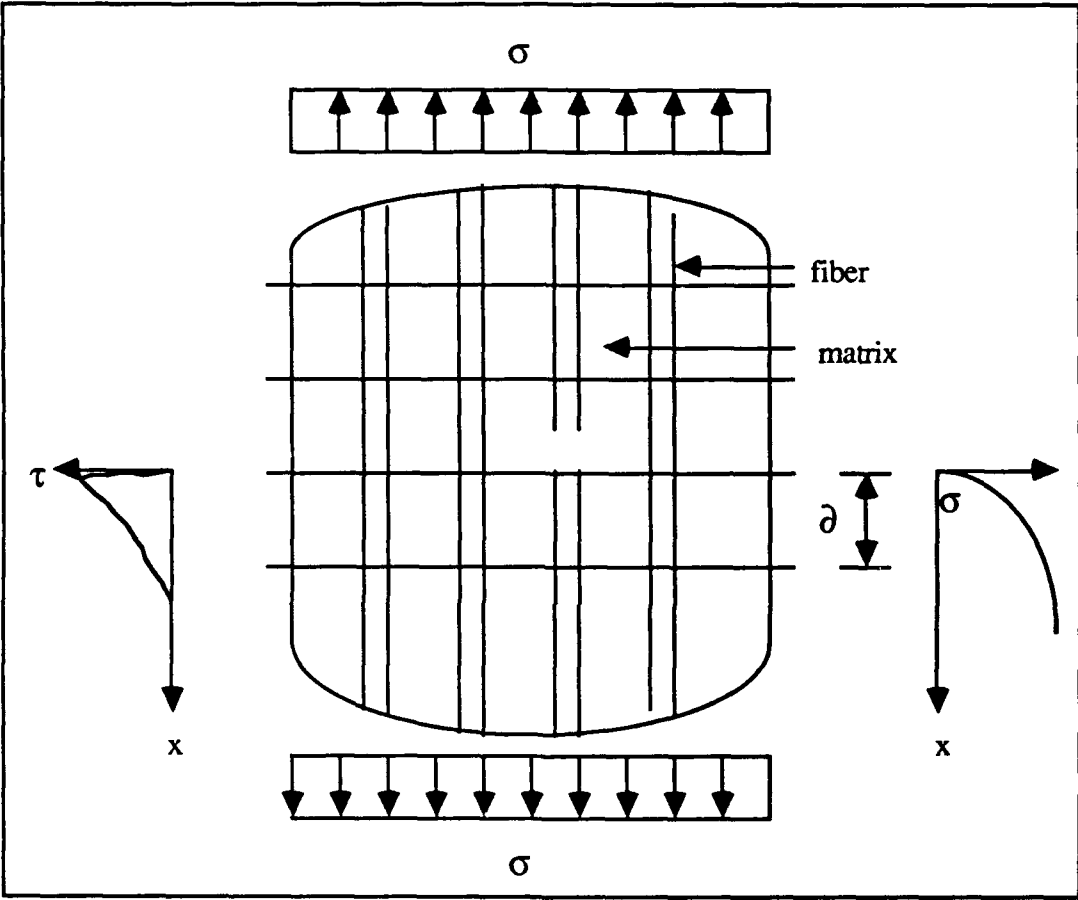
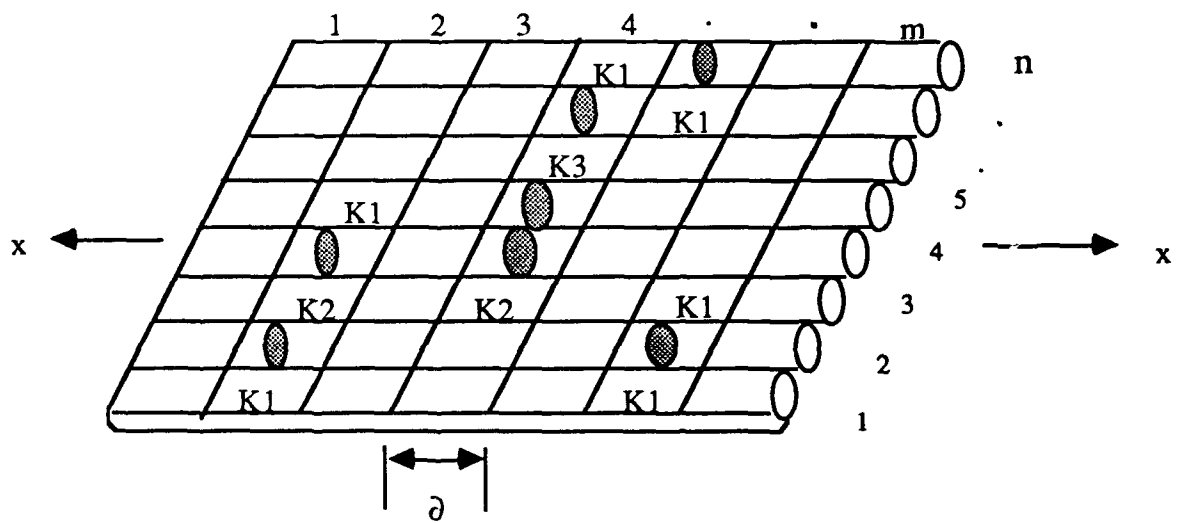


Figure 1. Composite Failure Model



X - Load Per Fiber
 ∂ - Fiber Element Length
 K_r - Load Concentration Factor
 N - Number Of Fibers
 M - Number Of Bundles

 - Fiber Break

Figure 2. Local Load Sharing Model

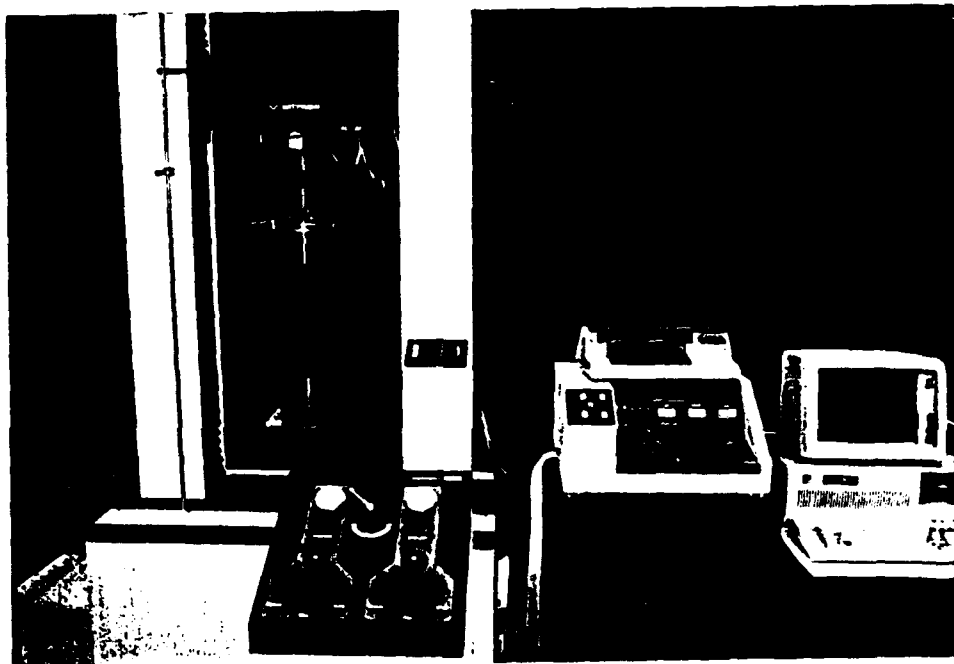


Figure 3. Instron Testing Instrument

Composit Strand Tensile (2 in. GL)

Report

Composit Strand Tensile (2 in. GL)

Report submenu
 Report header:
 Rep. header 2:
 Rep. header 3:
 Environmental parameters:
 Temperature to be entered: yes Defaults to : 24 degrees Celsius
 Humidity to be entered: yes Defaults to : 40 %
 User-defined fields:
 1 default
 2 default
 3 default
 4 default
 5 default
 Statistical analysis: enabled Minimum and maximum: yes
 Mean +/- std dev, yes set to +/- 2.00 Std. dev(s)
 Reduced report: enabled Report output default: printer
 Number of copies: 1

Data-collection

Composit Strand Tensile (2 in. GL)

4200/1011 Data collection submenu (4206)

Calibration: Reverse load polarity: no
 Sampling rate: 6.67 pt./sec.
 Handled by 4200/1011 disable reduct
 Load-cell used: 1000.00 Kgrams
 Begin data collection at: Computer
 Data compression: disabled
 Machine control parameters:
 disable test stop at:
 Test direction: up Xhead action at test end: stop
 Test end detection: delay: load threshold
 load: 10.0000 Kgrams
 High limits:
 HI load: 300.00 Kgrams HI extns: 20.00 mm

Figure 4. Test Method - 2" Gauge Length

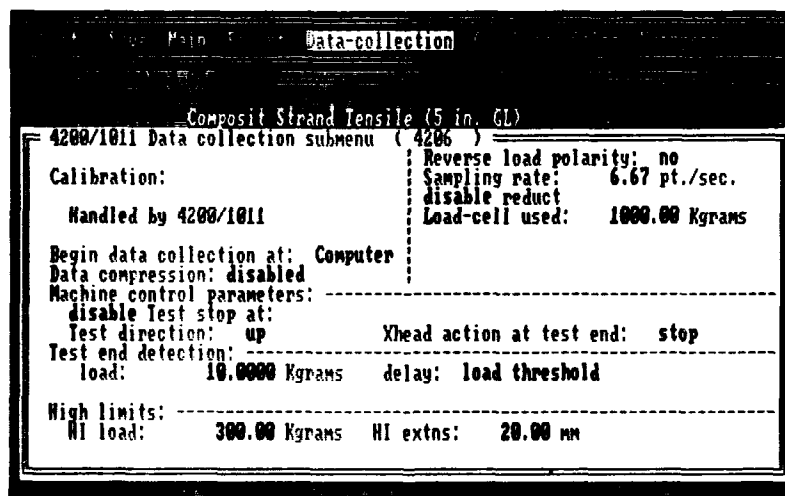
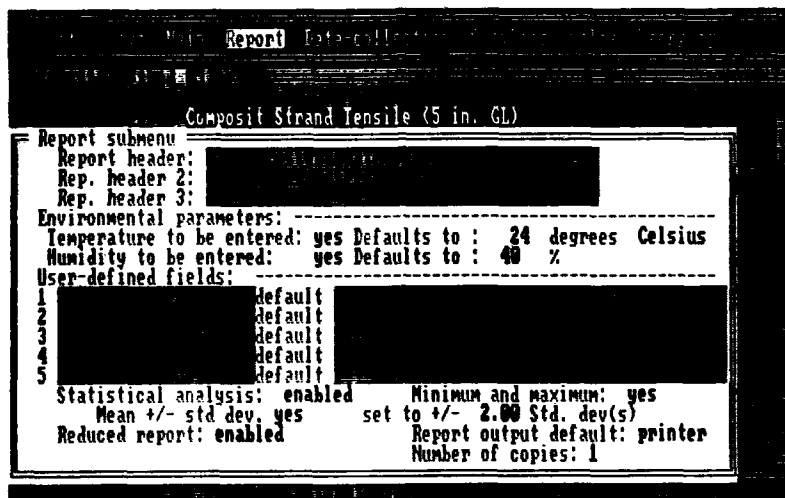
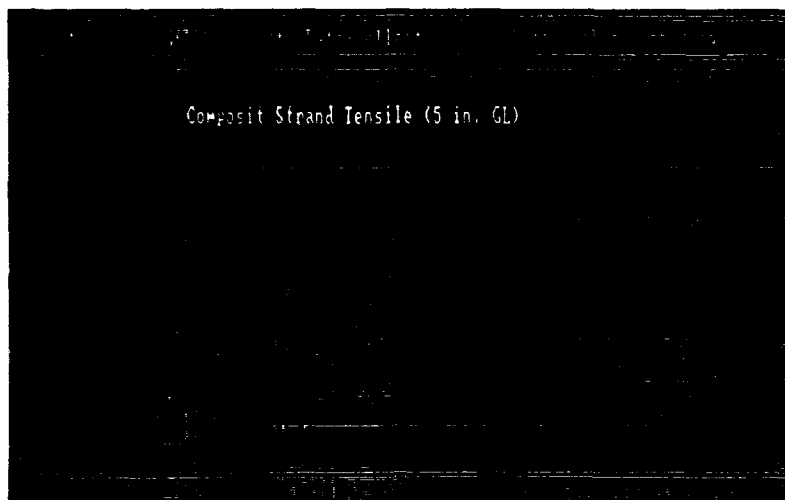


Figure 5. Test Method - 5" Gauge Length

```

Data-collection
Composit Strand Tensile (10 in. GL) - metric units
10 inch gauge length
reflected energy absorber utilized

```

```

Report
Composit Strand Tensile (10 in. GL) - metric units
Report submenu
Report header:
Rep. header 2:
Rep. header 3:
Environmental parameters:
Temperature to be entered: yes Defaults to : 24 degrees Celsius
Humidity to be entered: yes Defaults to : 40 %
User-defined fields:
1 default
2 default
3 default
4 default
5 default
Statistical analysis: enabled Minimum and maximum: yes
Mean +/- std dev. yes set to +/- 2.00 Std. dev(s)
Reduced report: enabled Report output default: printer
Number of copies: 1

```

```

Data-collection
Composit Strand Tensile (10 in. GL) - metric units
4200/1011 Data collection submenu ( 4206 )
Calibration:
Handled by 4200/1011
Begin data collection at: Computer
Data compression: disabled
Machine control parameters:
disable test stop at:
Test direction: up Xhead action at test end: stop
Test end detection:
load: 10.0000 Kgrams delay: load threshold
High limits:
HI load: 300.00 Kgrams HI extns: 20.00 mm
Reverse load polarity: no
Sampling rate: 6.67 pt./sec.
disable reduct
Load-cell used: 1000.00 Kgrams

```

Figure 6. Test Method - 10" Gauge Length

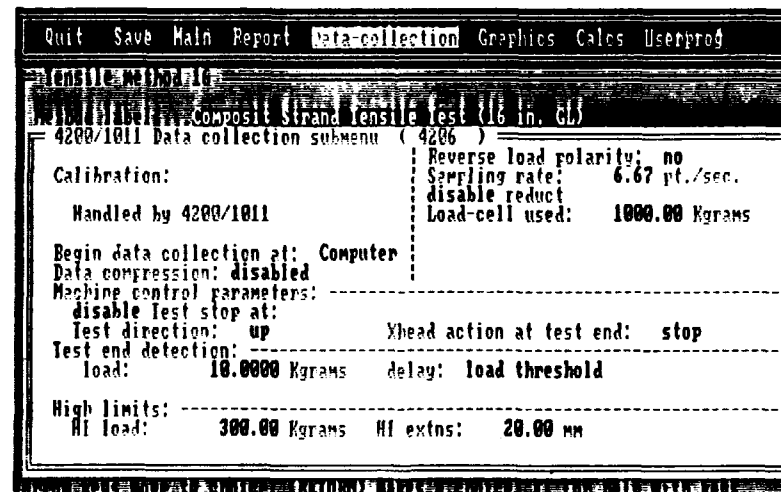
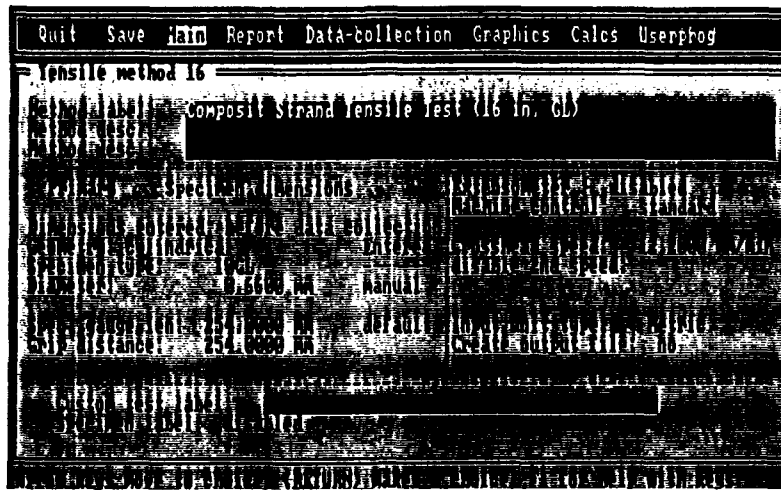


Figure 7. Test Method - 16" Gauge Length

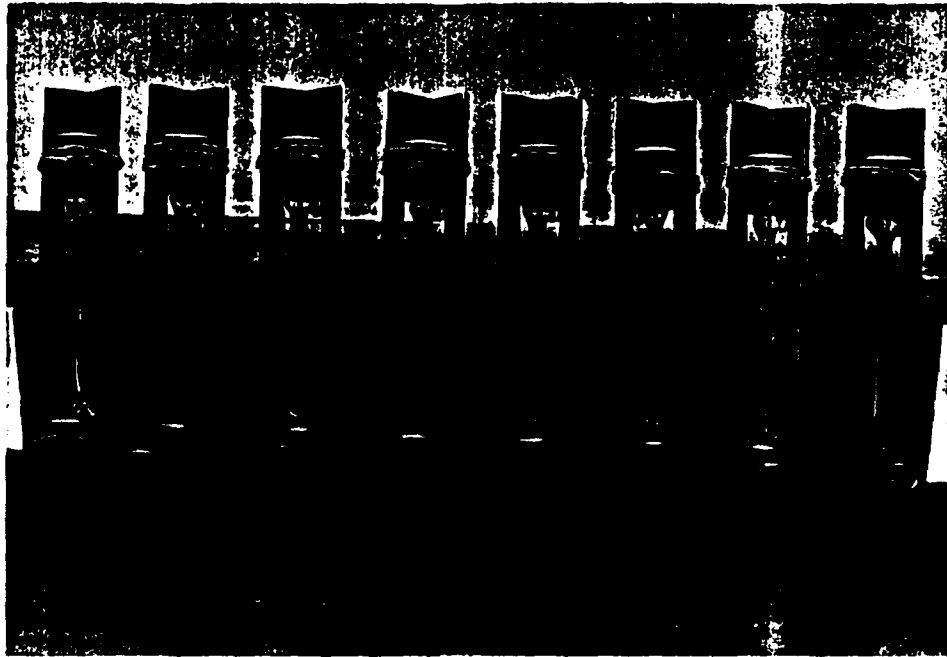


Figure 8. Composite Strand Test Samples

Naval Postgraduate School
Composites Material Lab
Thesis - Johnson

Sample Identification: 00816-01

Test Date: April 11, 1991

Out of 1 specimens, 0 excluded.

Sample comments: Very good break, ends intact, rest shattered.

Specimen Number	Displacement	Load	Stress	Strain	% Strain	Displacement	Load	Stress	Strain
	at Max. Load (mm)	at Max. Load (Kg)	at Max. Load (Kg/mm ²)	at Max. Load (mm/mm)	at Max. Load (%)	at Auto. Break (mm)	at Auto. Break (Kg)	at Auto. Break (Kg/mm ²)	at Auto. Break (mm/mm)
1	7.130	53.42	156.1	.02807	2.807	7.130	53.42	156.1	.02807
Mean:	7.130	53.42	156.1	.02807	2.807	7.130	53.42	156.1	.02807
Standard Deviation:	-----	-----	-----	-----	-----	-----	-----	-----	-----
Mean - 2.00 * Sdv:	-----	-----	-----	-----	-----	-----	-----	-----	-----
Mean + 2.00 * Sdv:	-----	-----	-----	-----	-----	-----	-----	-----	-----
Minimum:	7.130	53.42	156.1	.02807	2.807	7.130	53.42	156.1	.02807
Maximum:	7.130	53.42	156.1	.02807	2.807	7.130	53.42	156.1	.02807

Specimen Number	% Strain at Auto. Break (%)	Modulus (Kg/mm ²)
	1	2.807
Mean:	2.807	5897.
Standard Deviation:	-----	-----
Mean - 2.00 * Sdv:	-----	-----
Mean + 2.00 * Sdv:	-----	-----
Minimum:	2.807	5897.
Maximum:	2.807	5897.

Figure 9. Sample Test Report

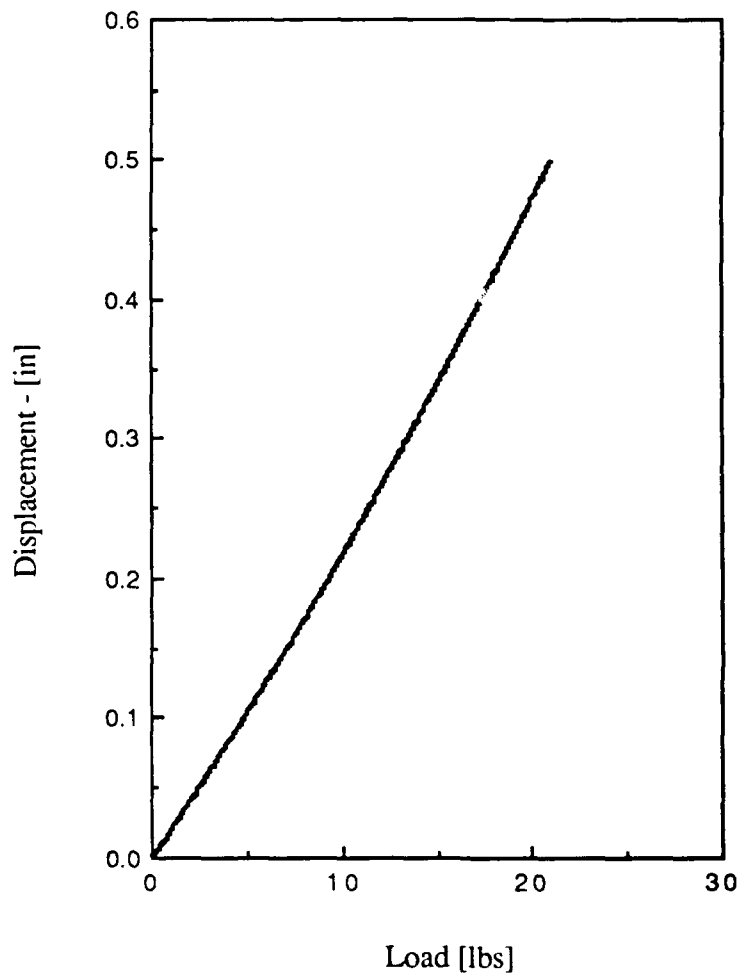


Figure 10. Hot-Melt Adhesive Load Displacement Data

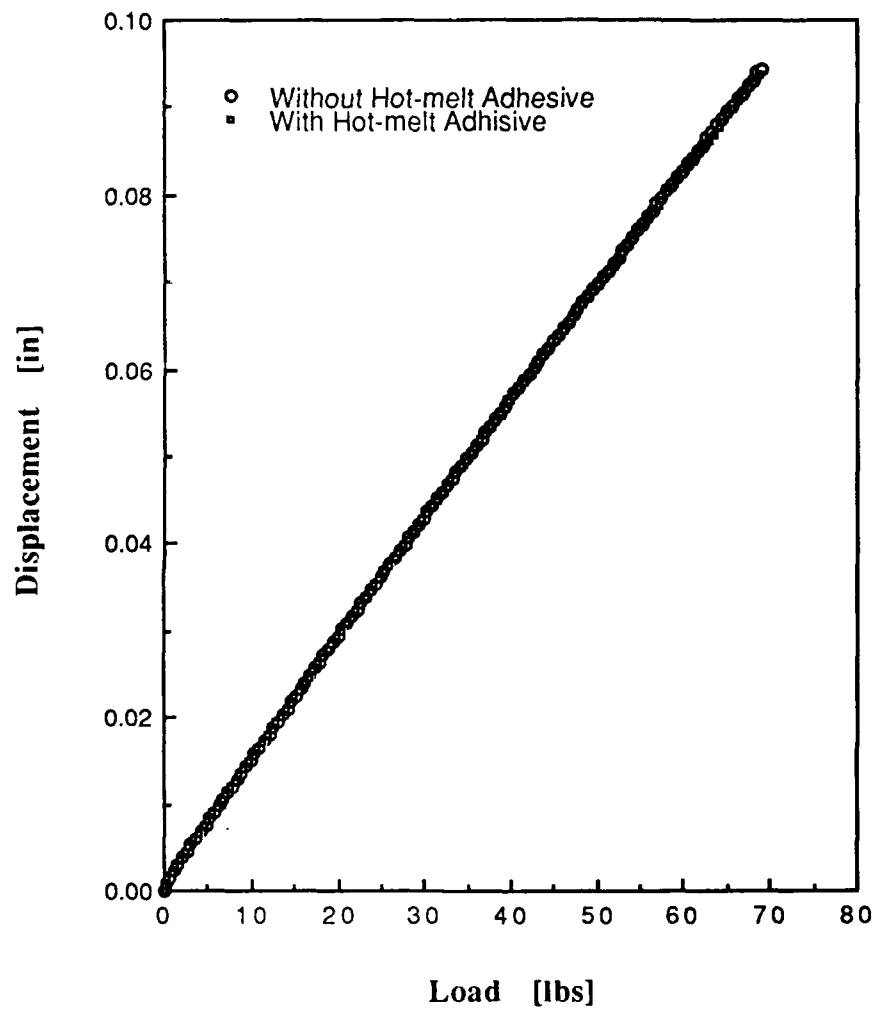


Figure 11. Load-Deformation Comparison of Hot-Melt Adhesive

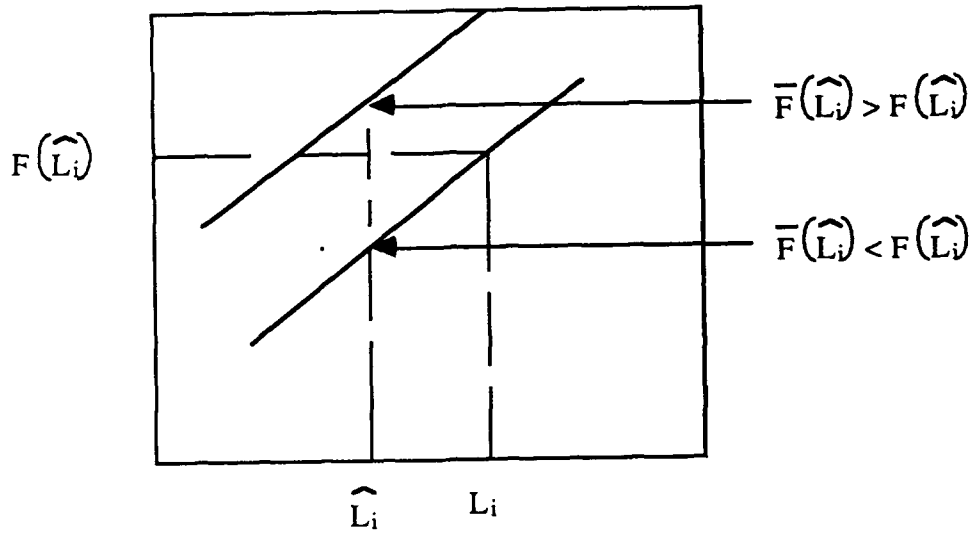
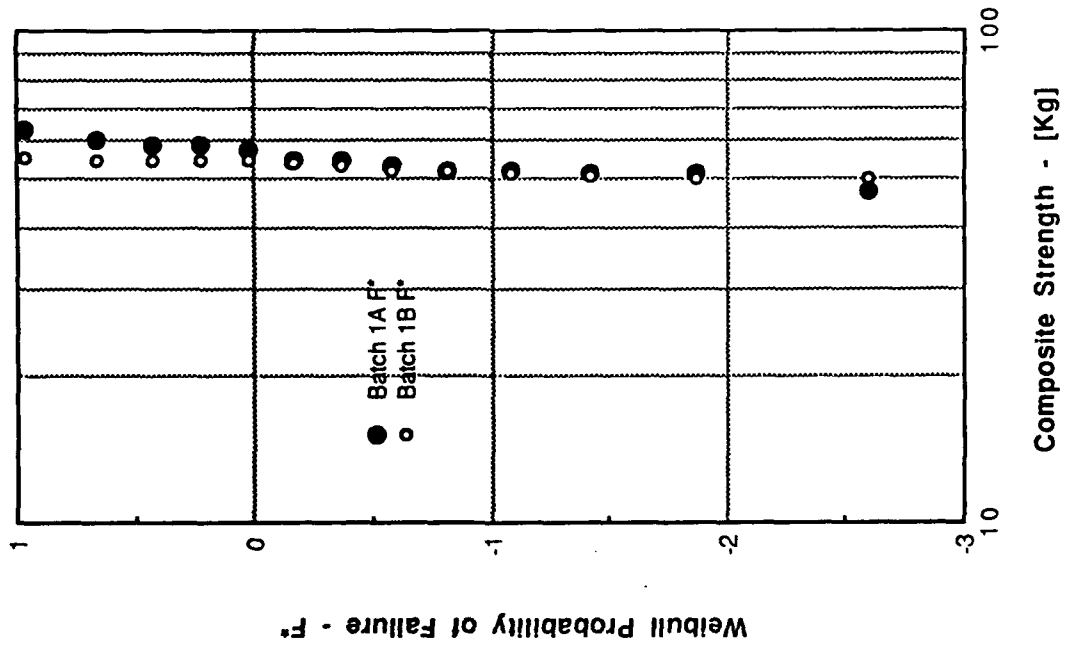


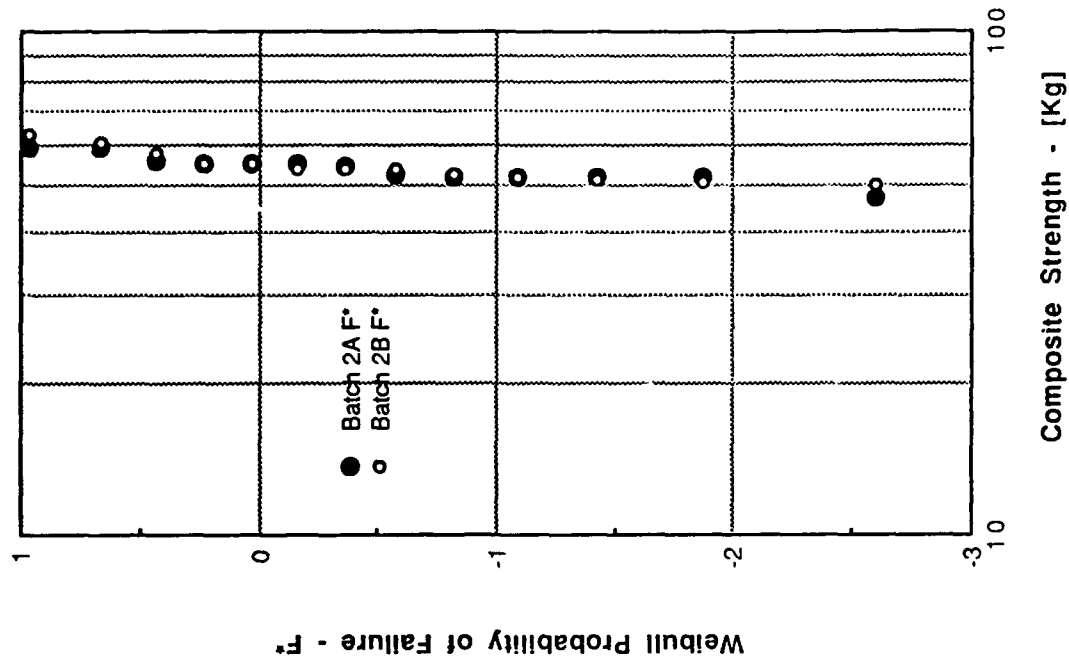
Figure 12. MLE Probability Shift

019 2" Batch 1 Band Width



(a)

019 2" Batch 2 Band Width



(b)

Figure 13. 019 2" Band Width Comparison

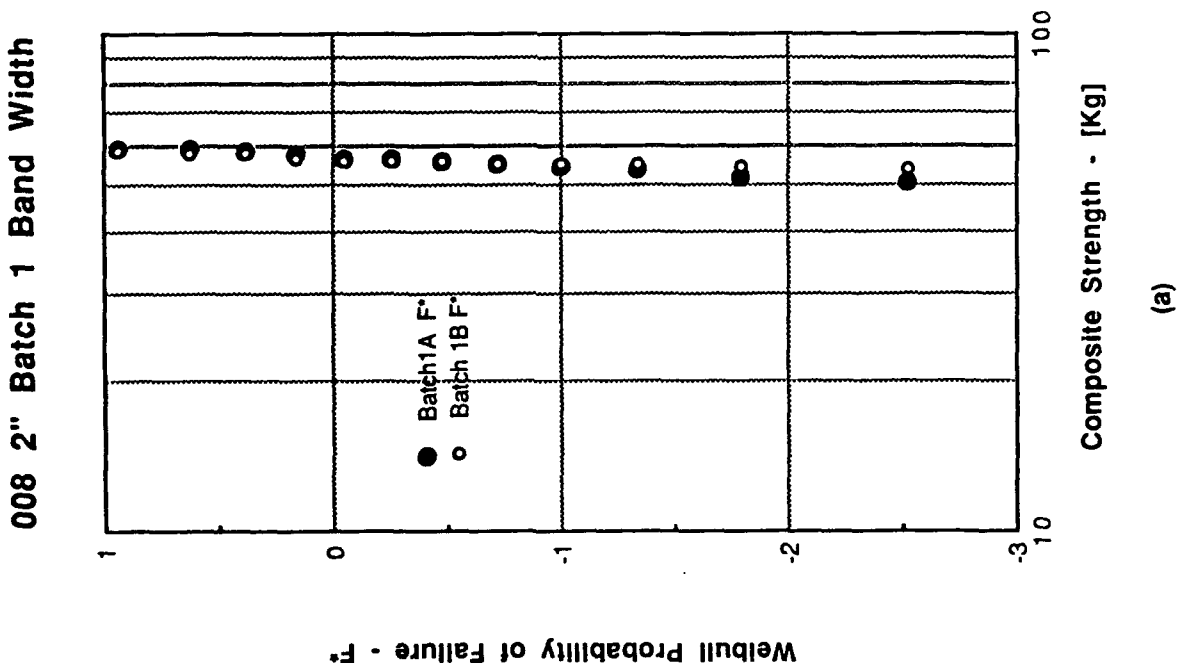
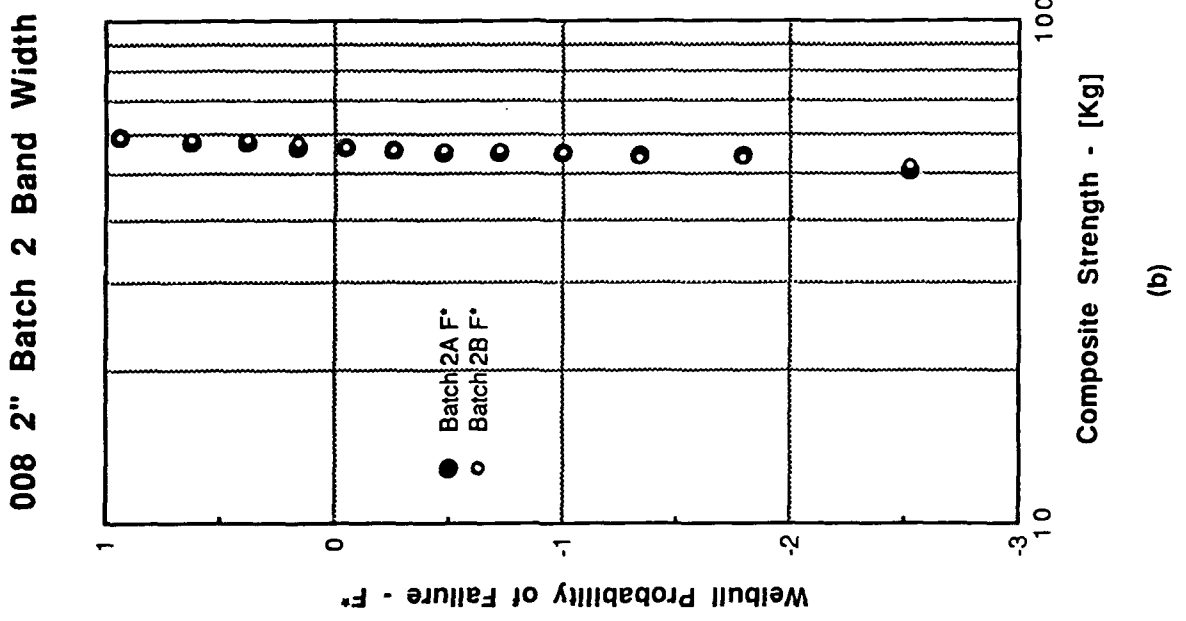


Figure 14. 008 2" Band Width Comparison

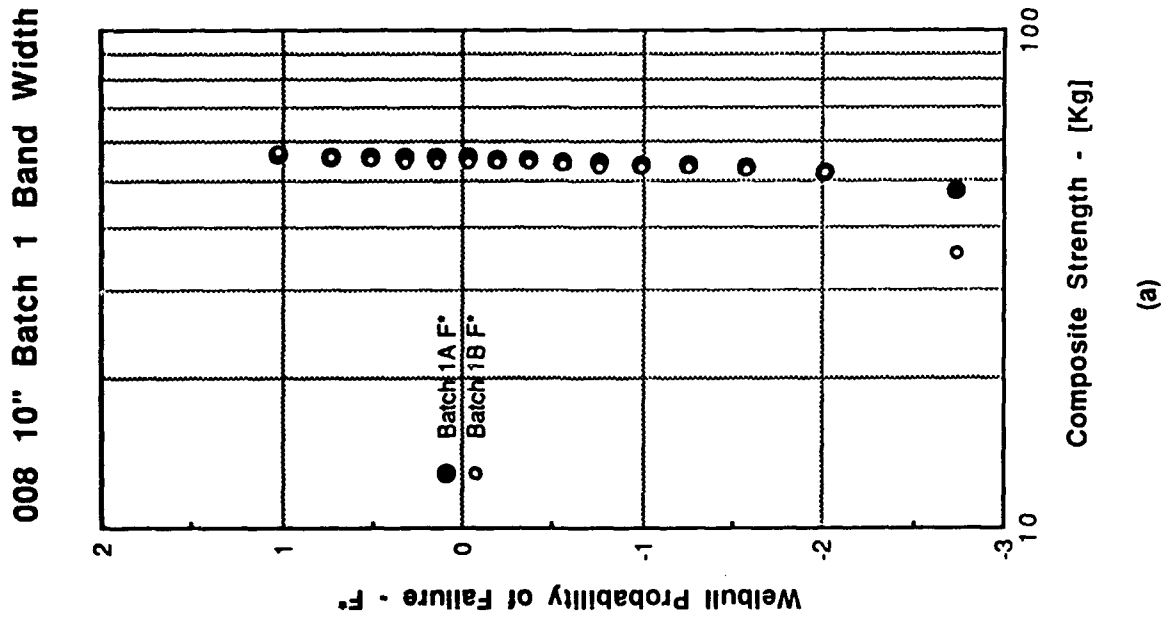
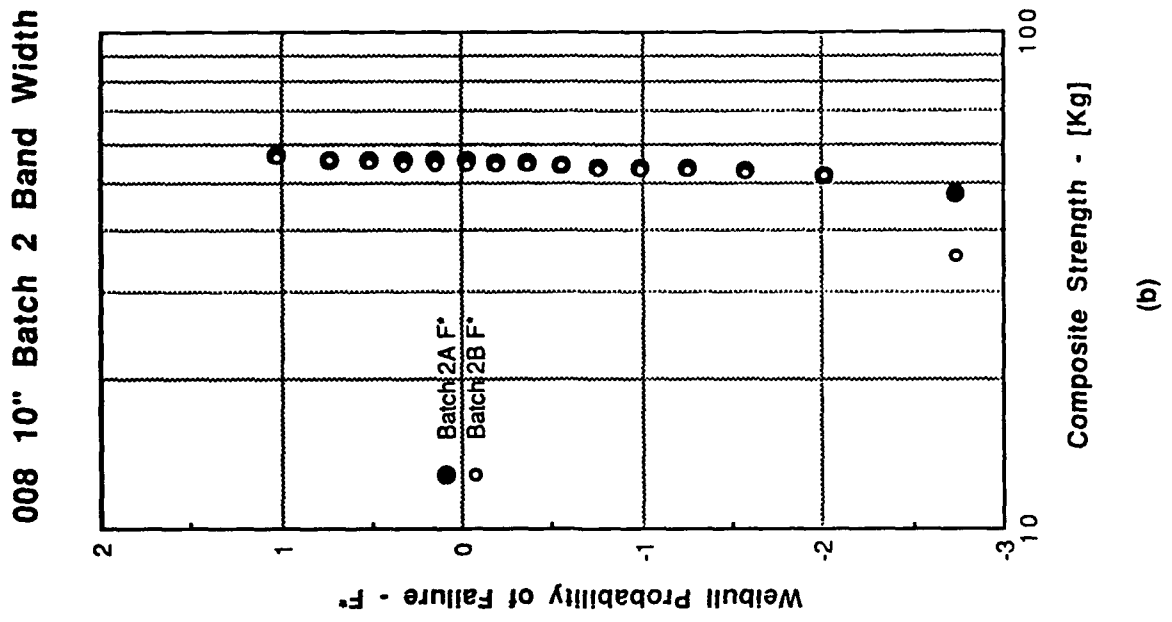


Figure 15. 008 10" Band Width Comparison

019 2" Weibull Model - Merged Data Comparison

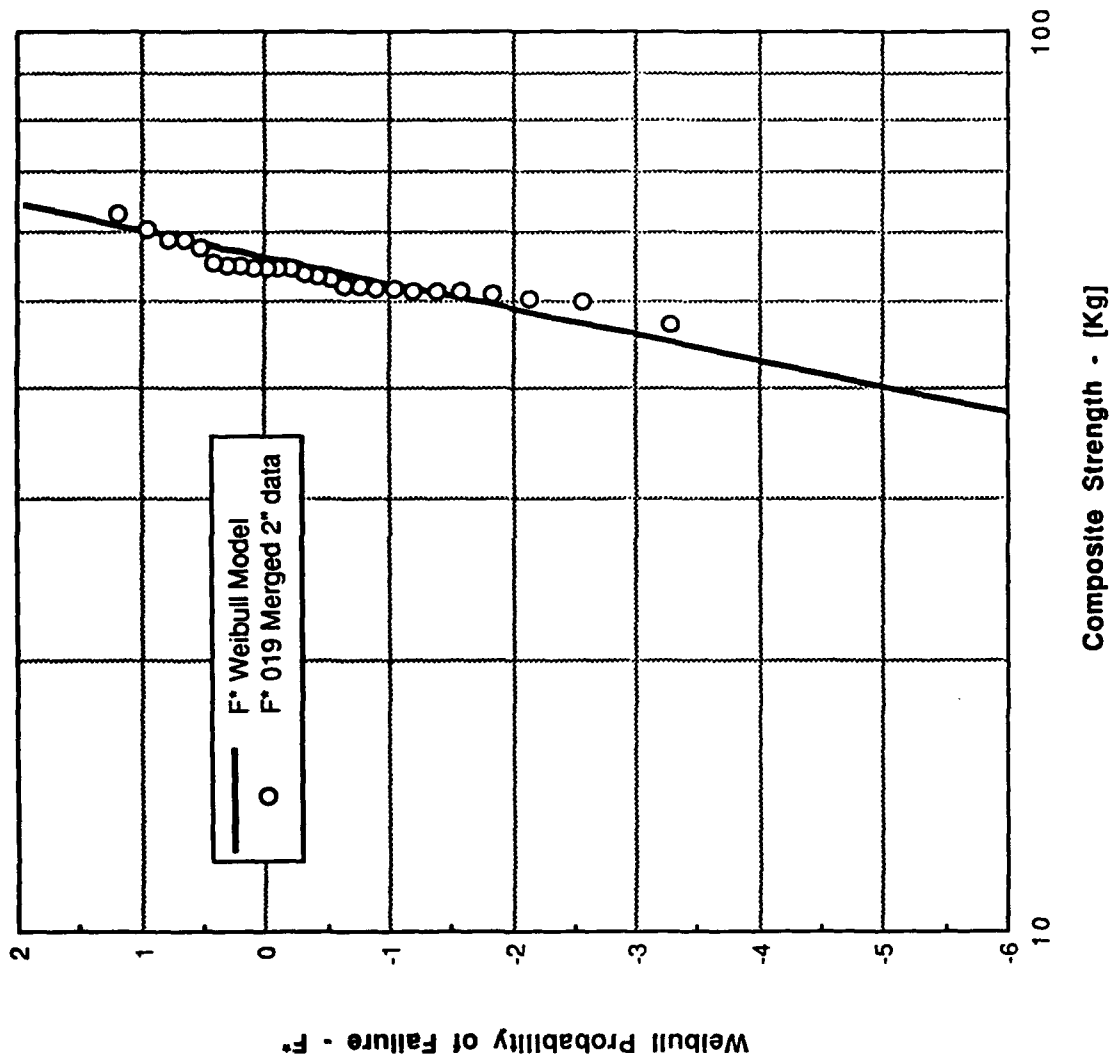


Figure 16. 019 2" Weibull Model-Merged Composite Data Comparison

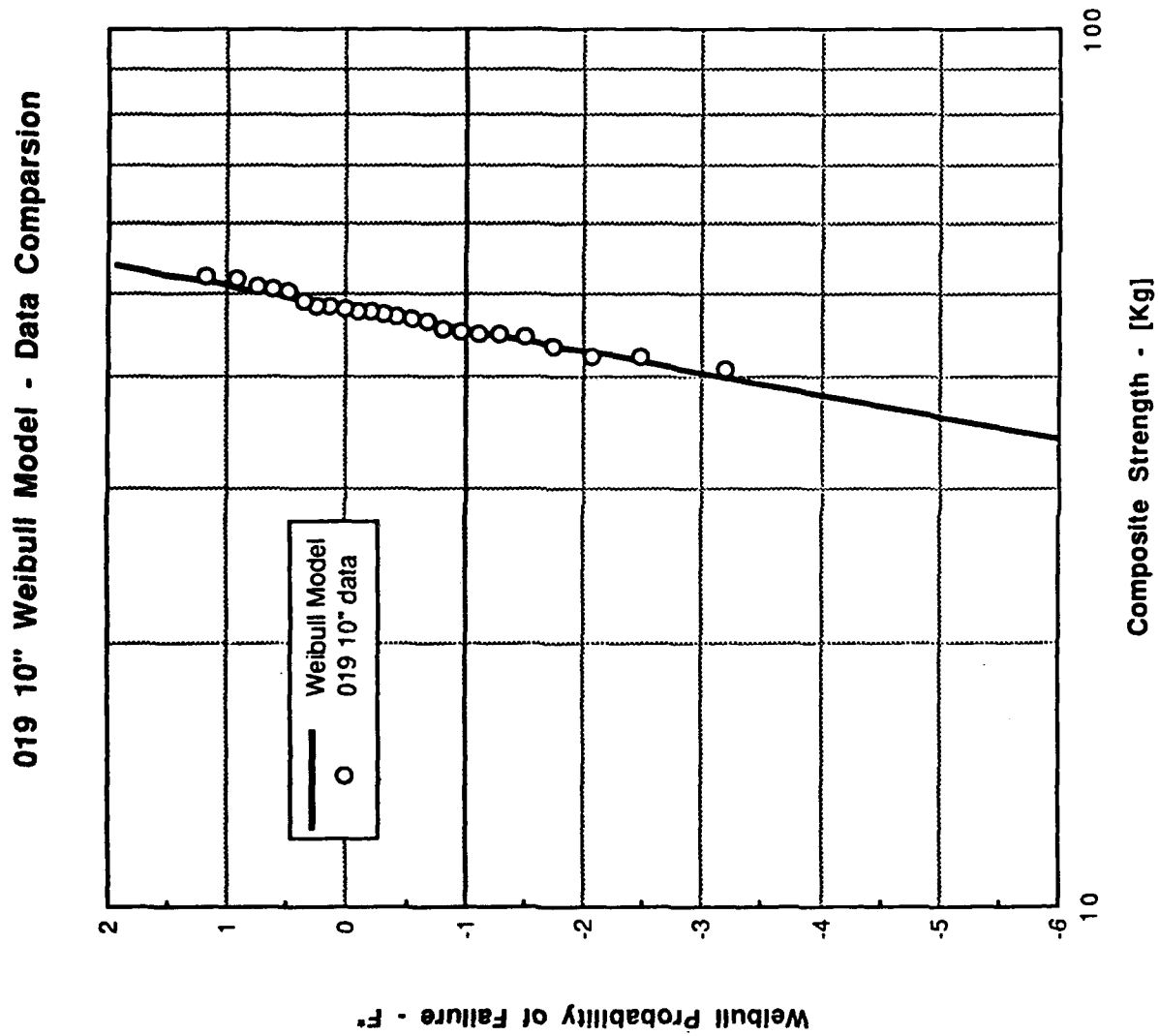


Figure 17. 019 10" Weibull Model-Composite Data Comparison

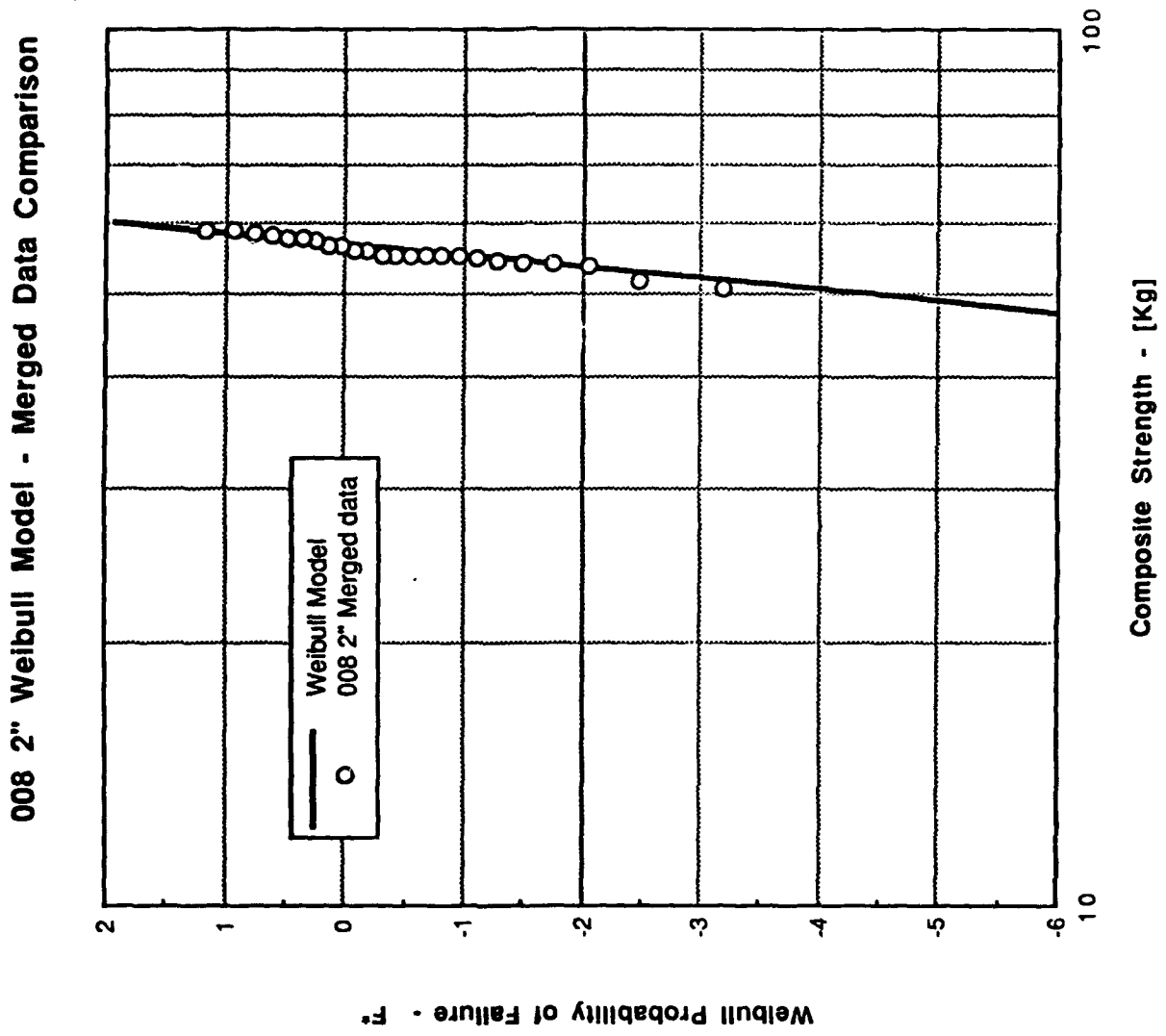


Figure 18. 008 2" Weibull Model-Merged Composite Data Comparison

008 10" Set A Weibull Model Data Comparison

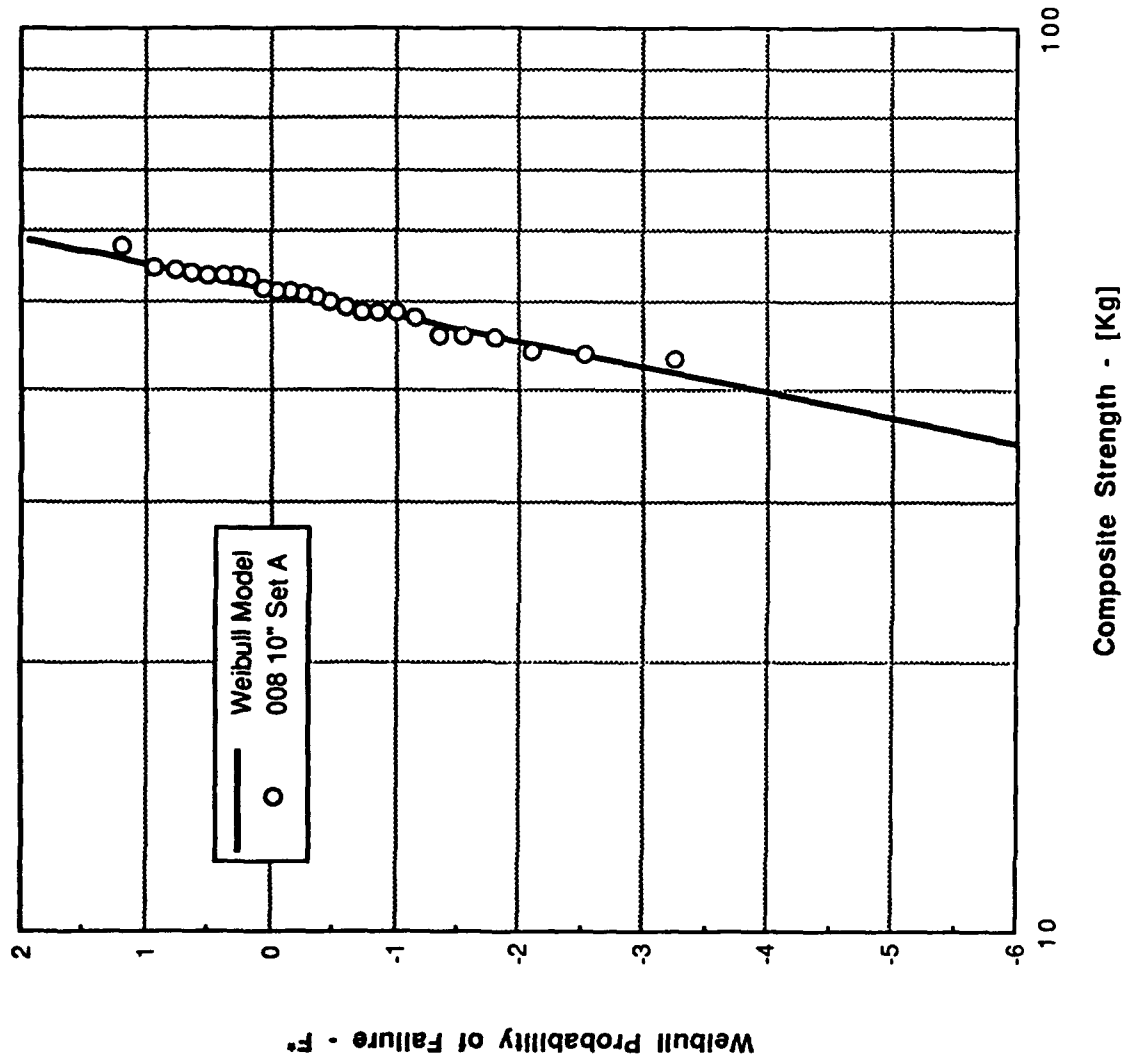


Figure 19. 008 10" Set A Weibull Model-Merged Composite Data Comparison

008 10" Set B Weibull Model Data Comparison

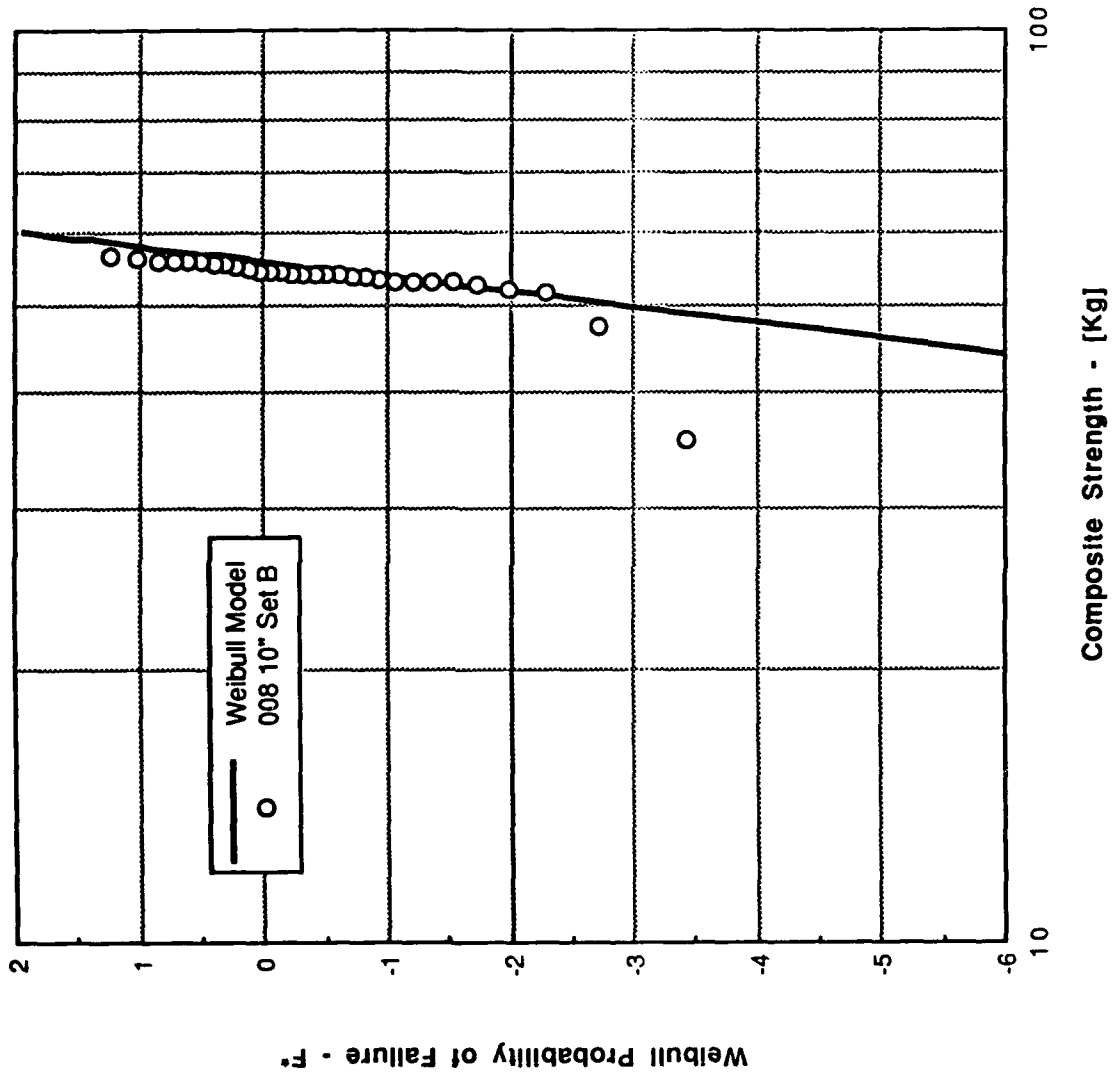


Figure 20. 008 10" Set B Weibull Model-Merged Composite Data Comparison

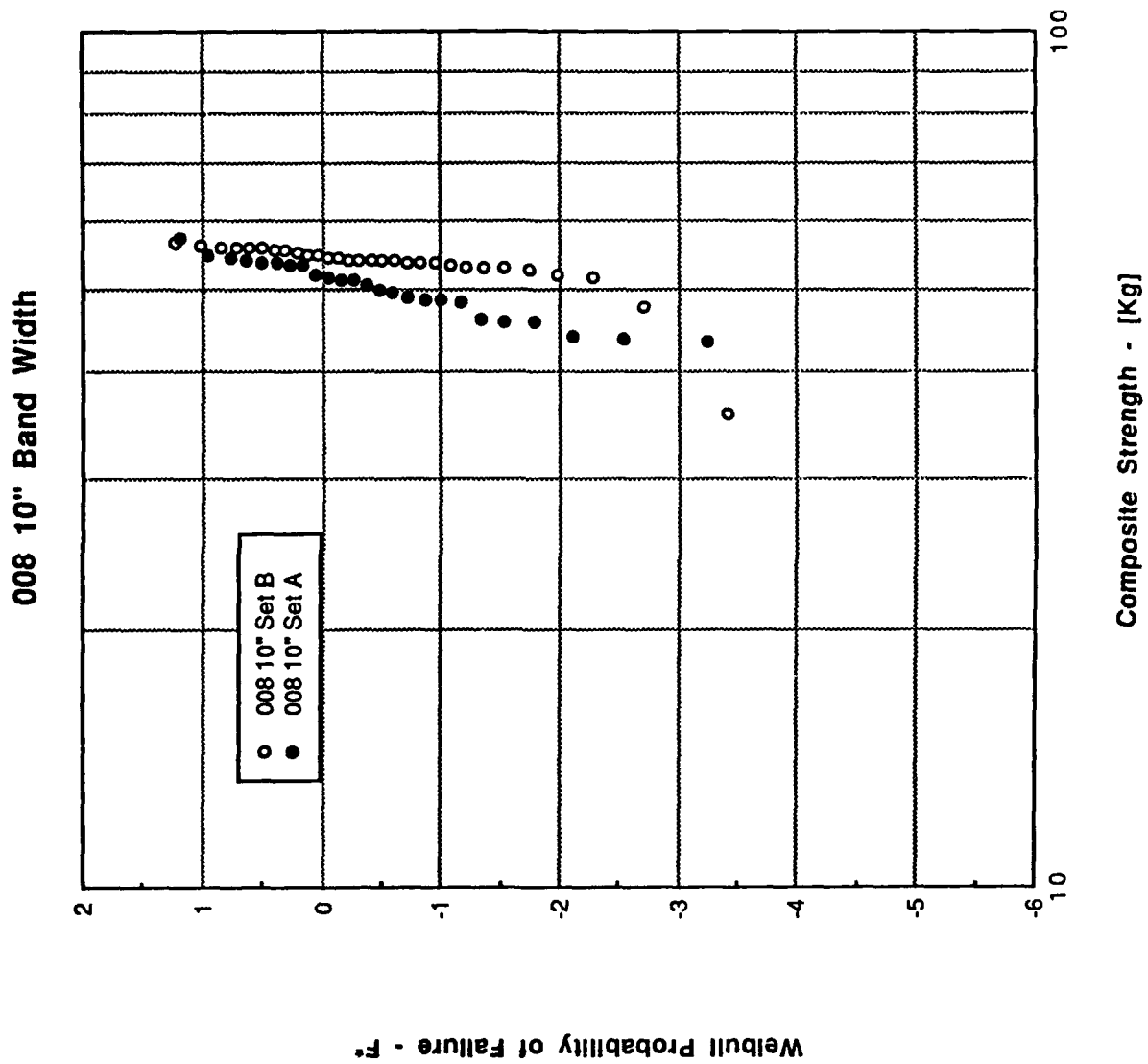


Figure 21. 008 10" Composite Band Width Comparison

008 All 10" Merged Weibull Model
Data Comparison

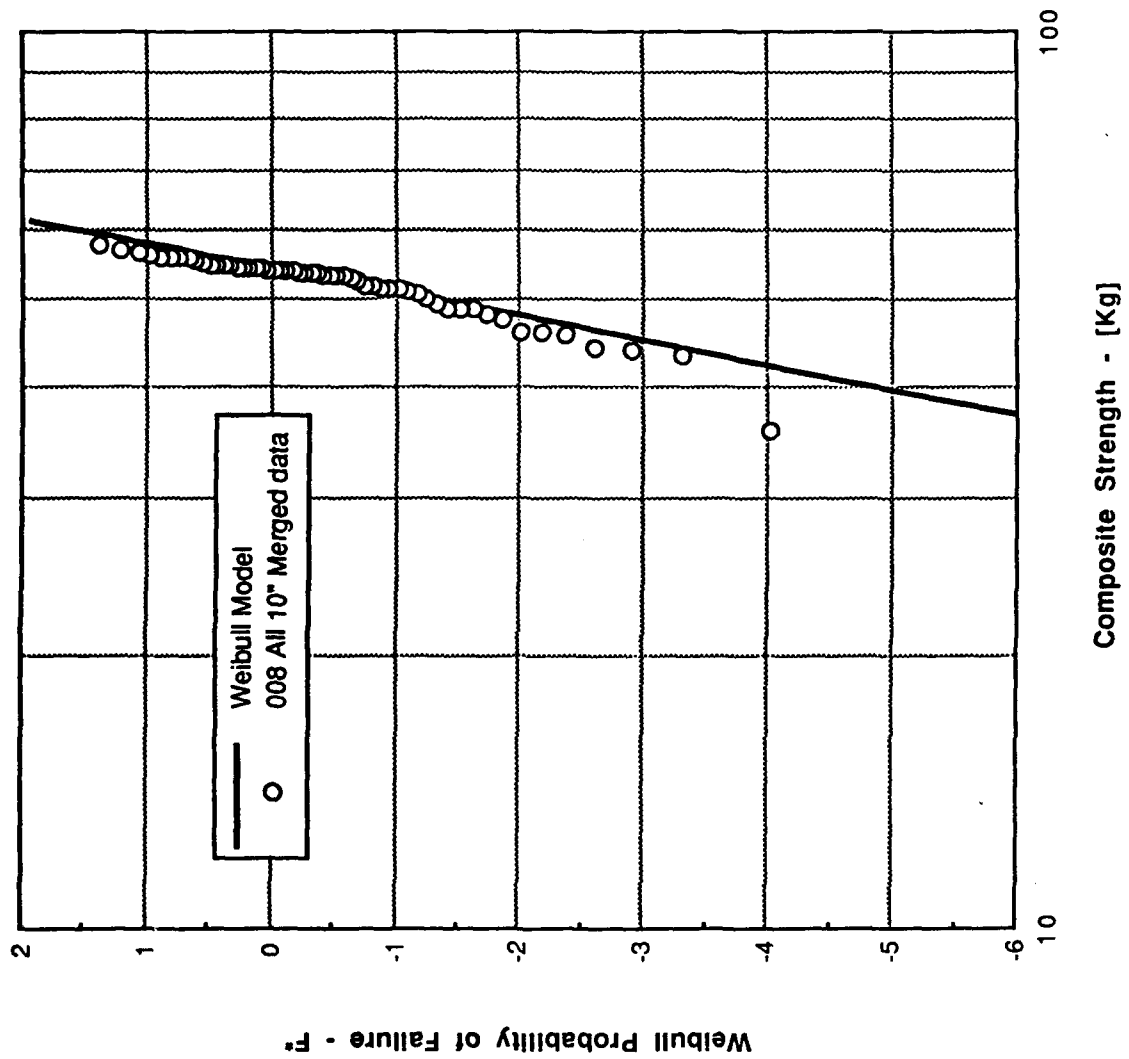


Figure 22. 008 (All) 10" Weibull Model-Merged Composite Data Comparison

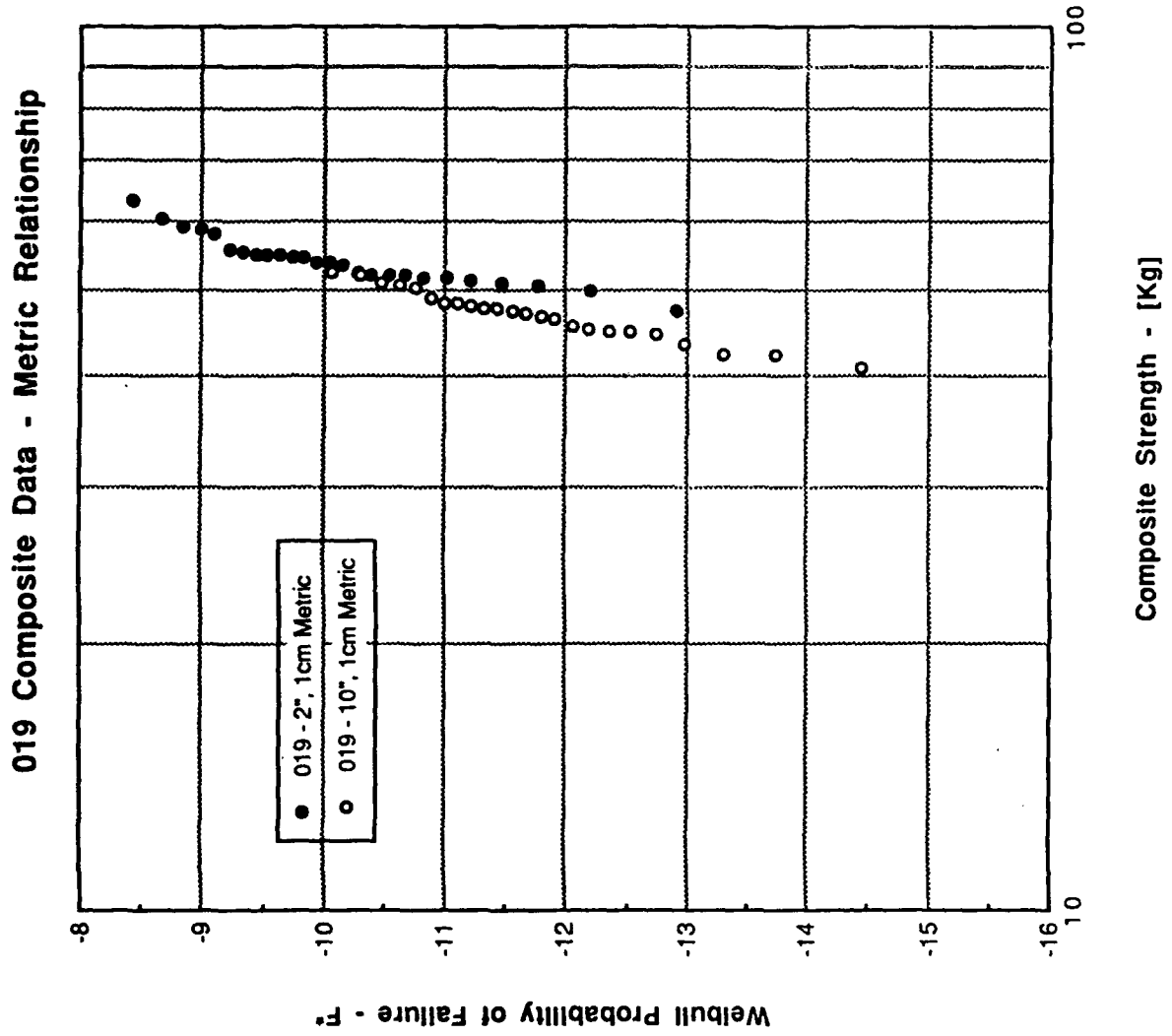


Figure 23. 019 Composite Data-Metric Relationship

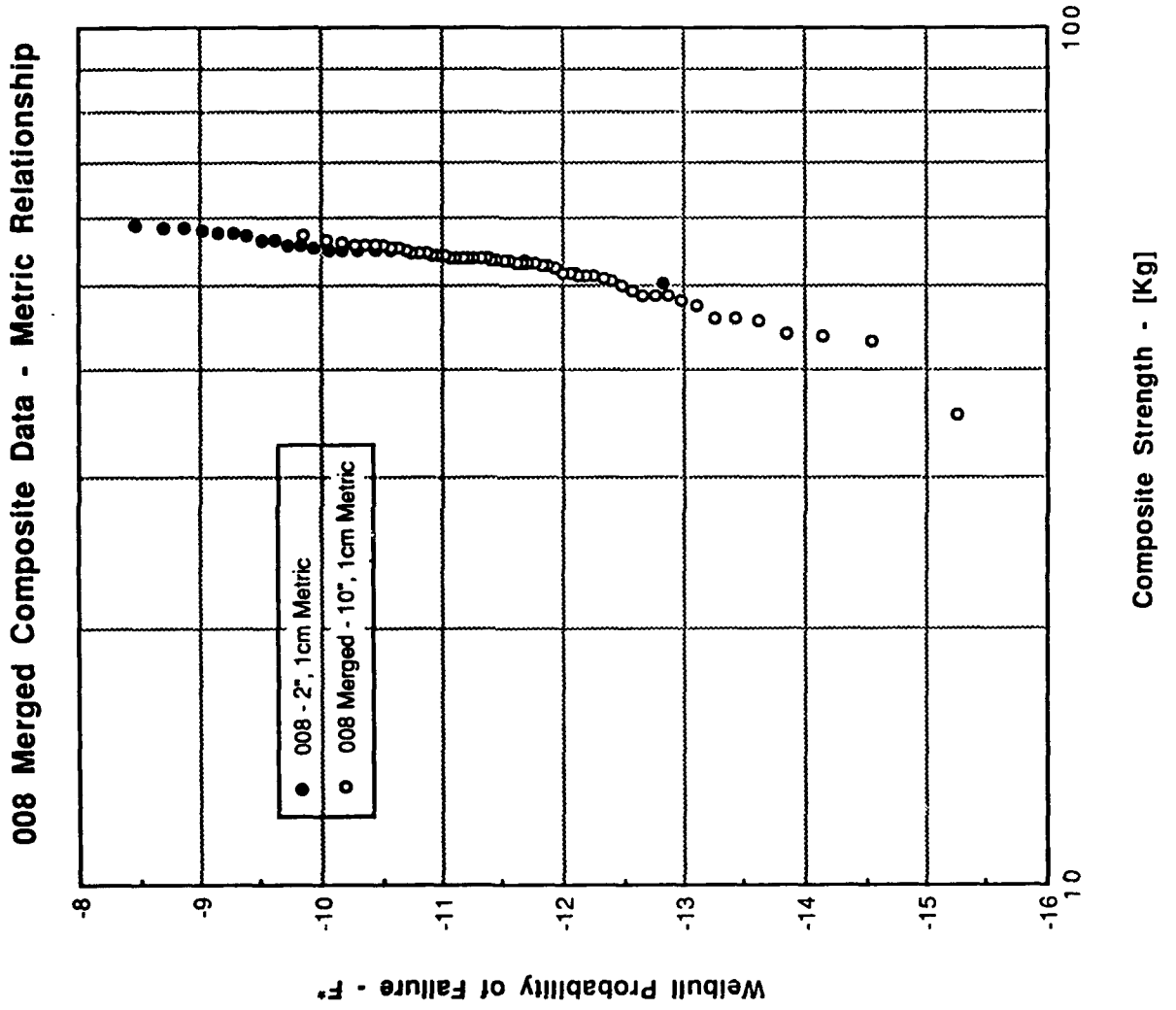


Figure 24. 008 Merged Composite Data-Metric Relationship

019 Composite Data (per fiber) - Metric Relationship

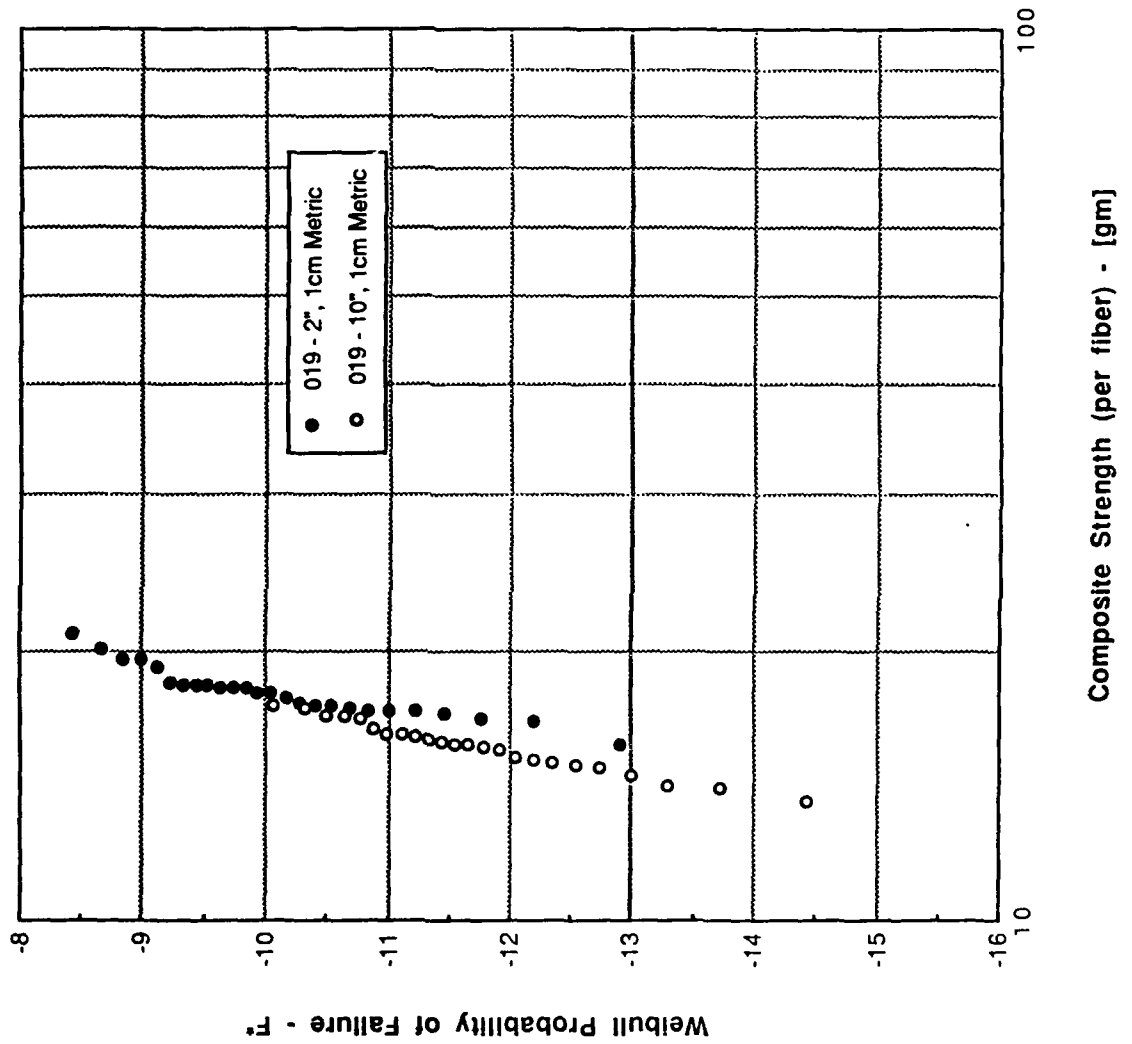


Figure 25. 019 Composite Data (per fiber)-Metric Relationship

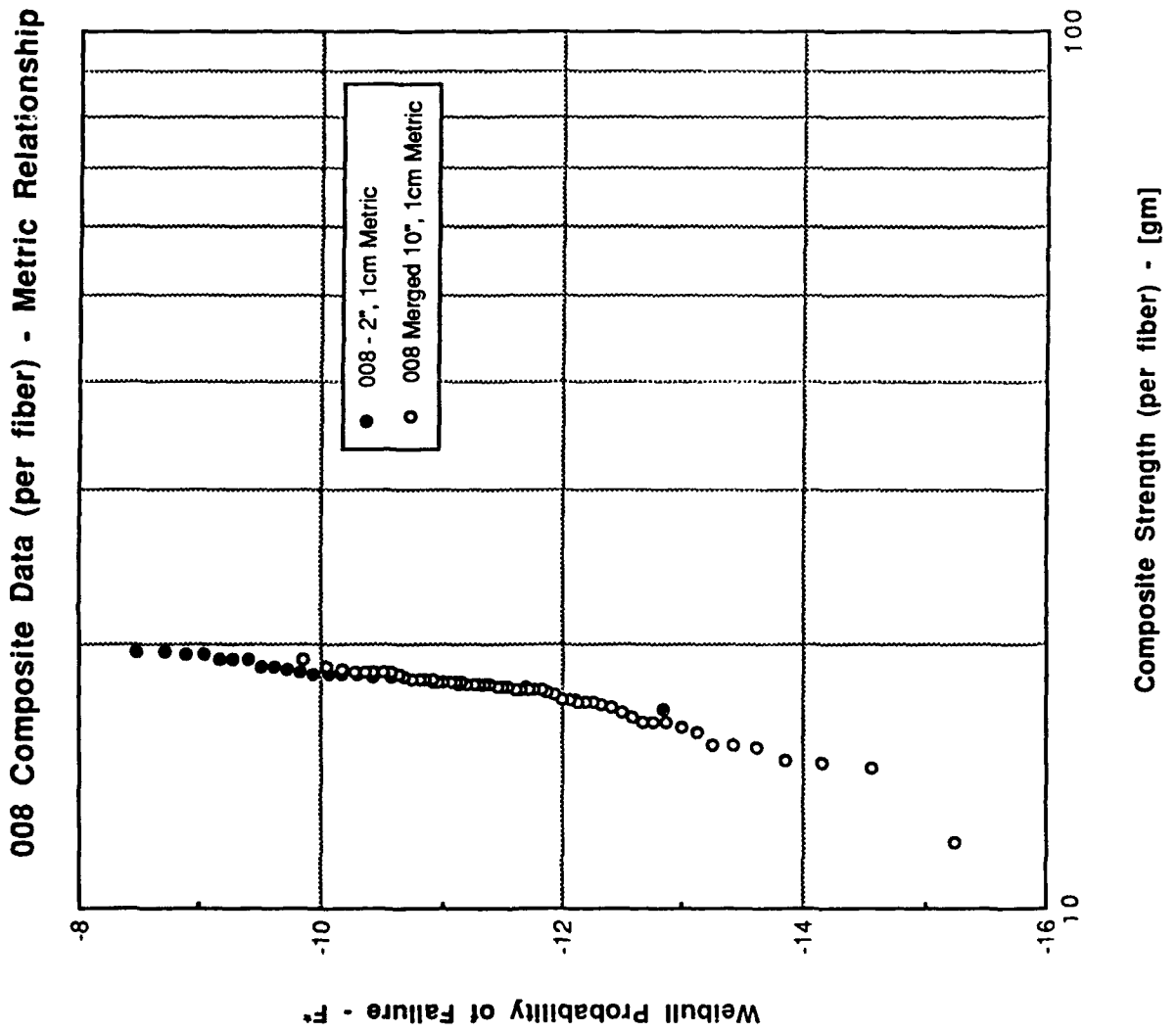


Figure 26. 008 Composite Data (per fiber)-Metric Relationship

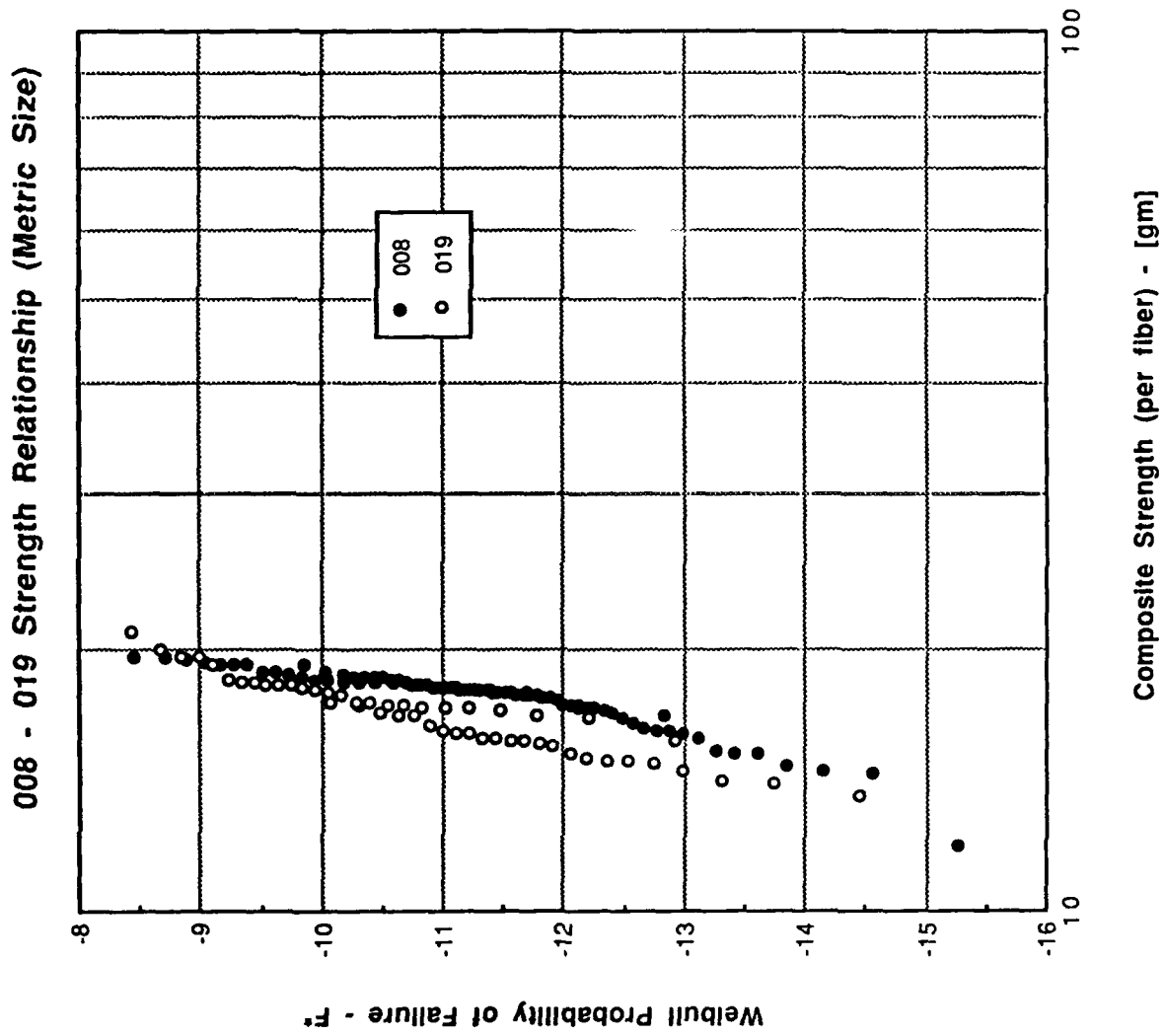


Figure 27. 008-019 Composite Strength Relationship

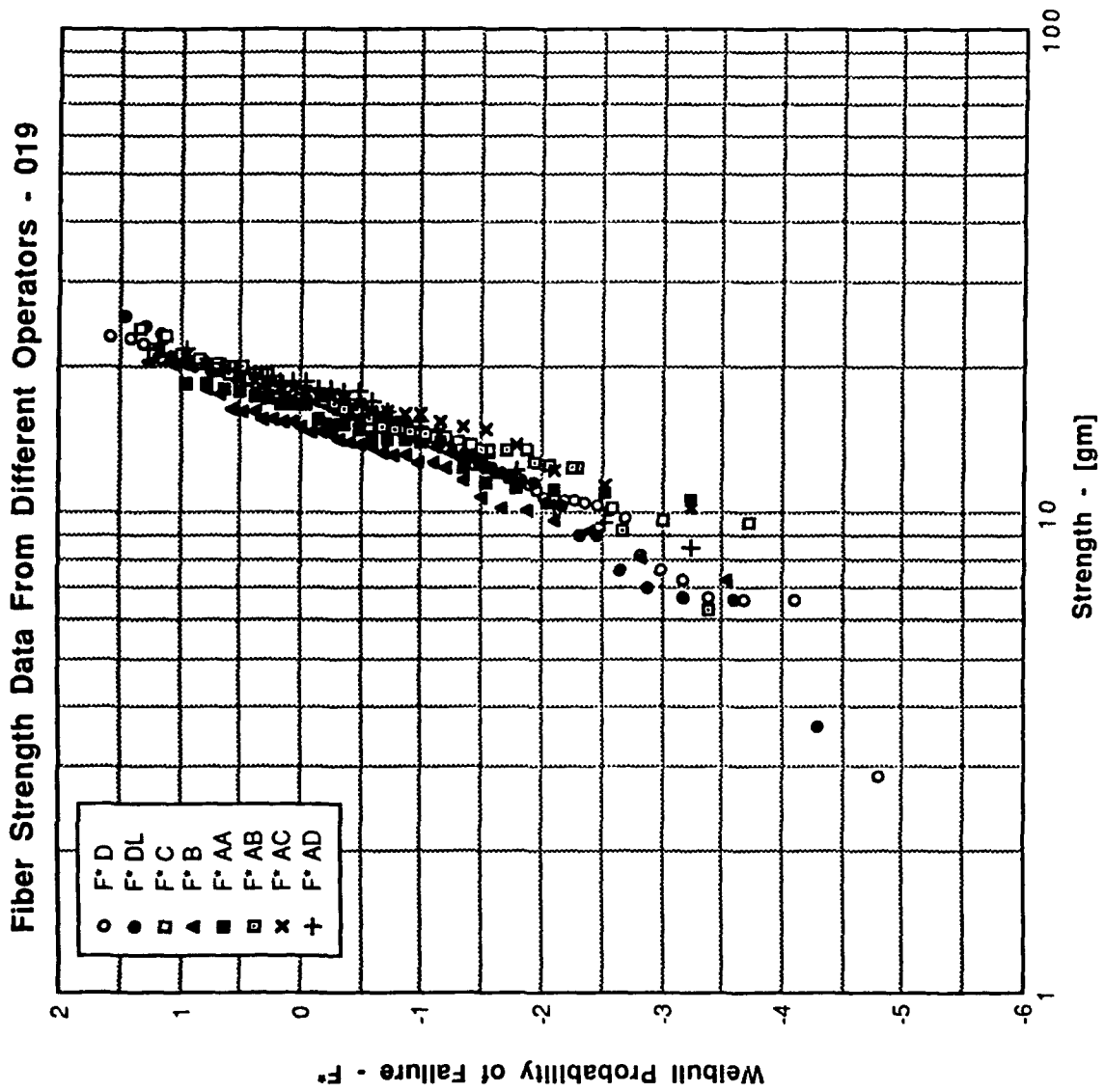


Figure 28. 019 Fiber Data Band Width Comparison

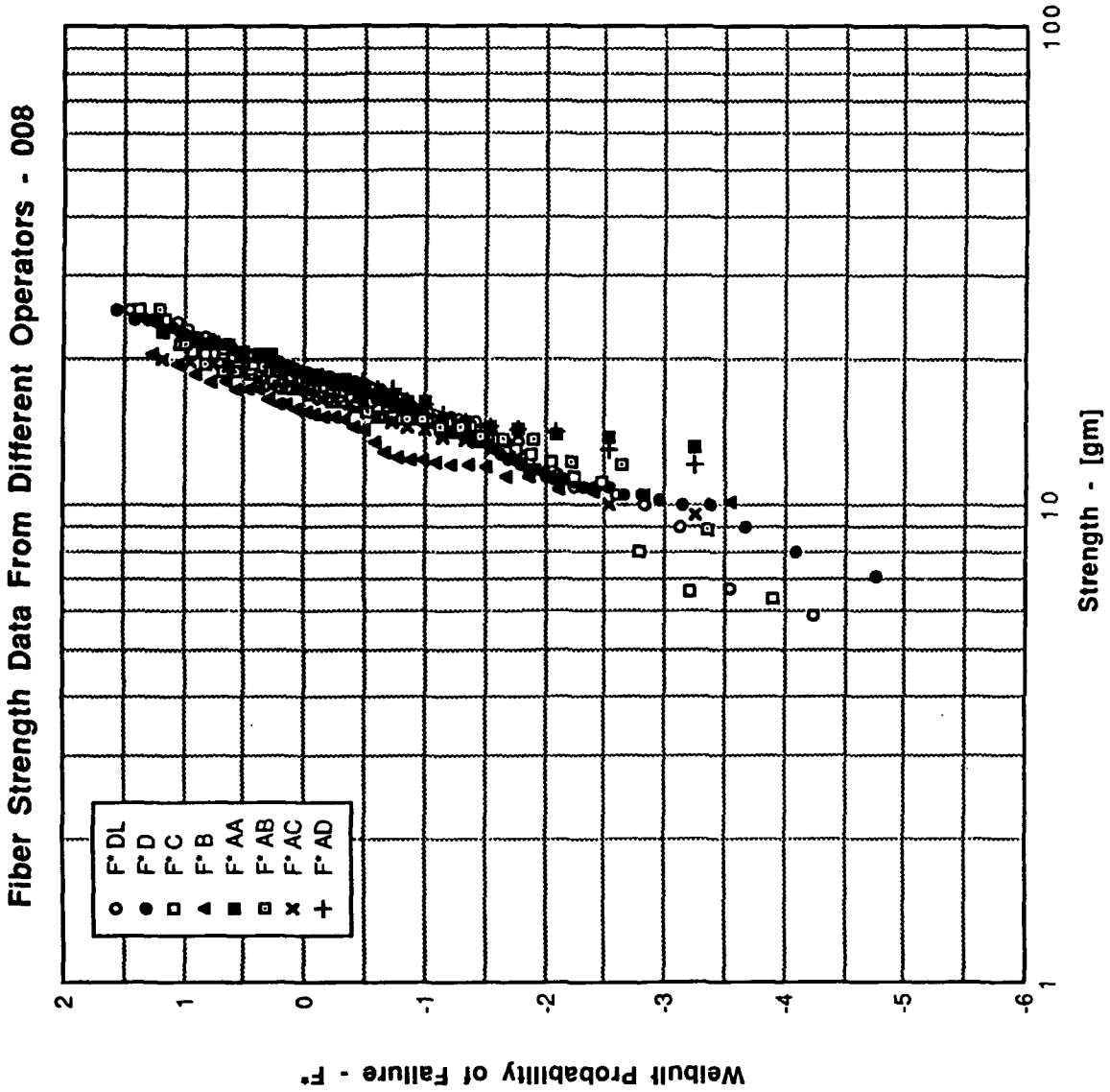


Figure 29. 008 Fiber Data Band Width Comparison

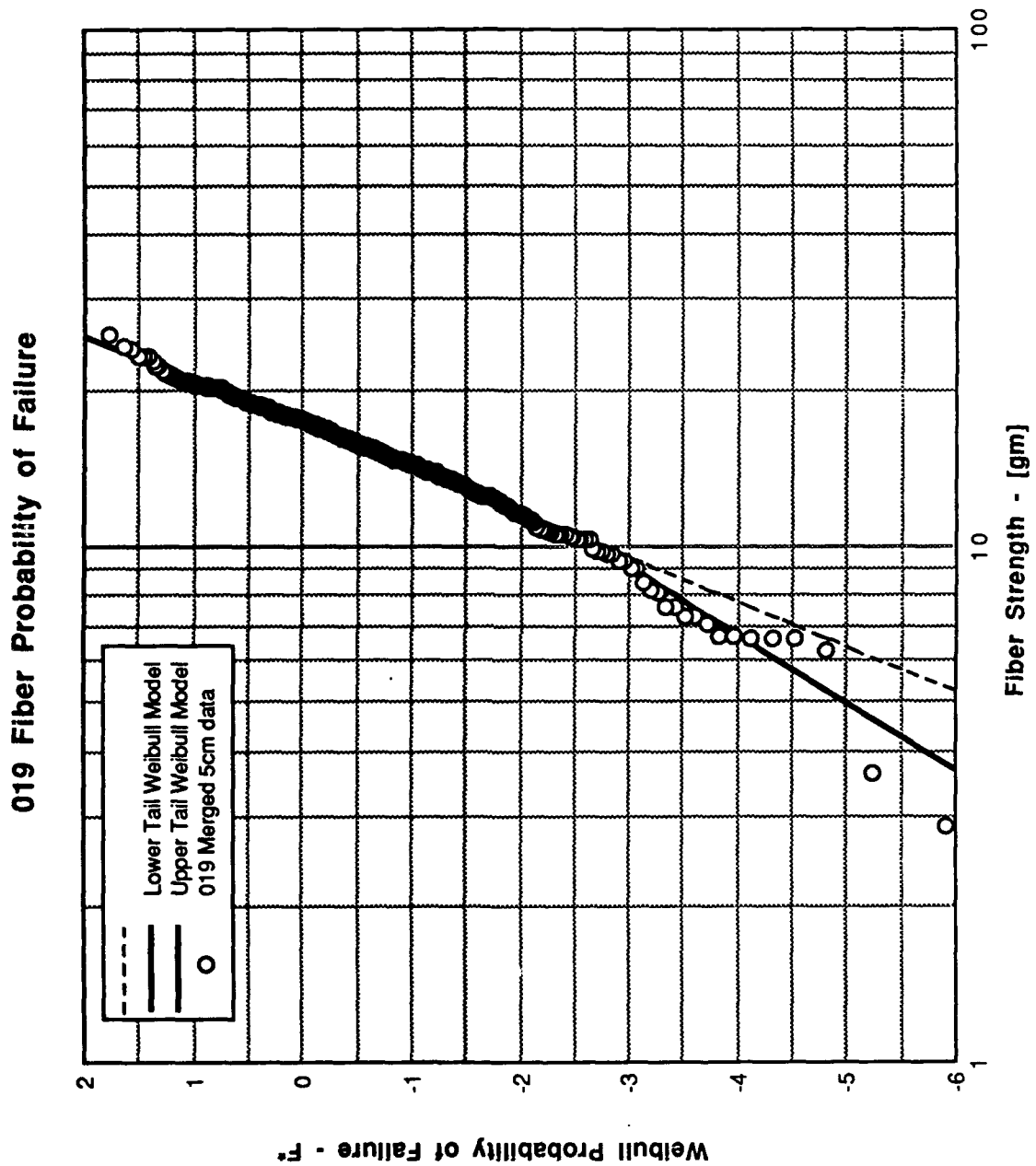


Figure 30. 019 Weibull Model-Merged Fiber Data Comparison

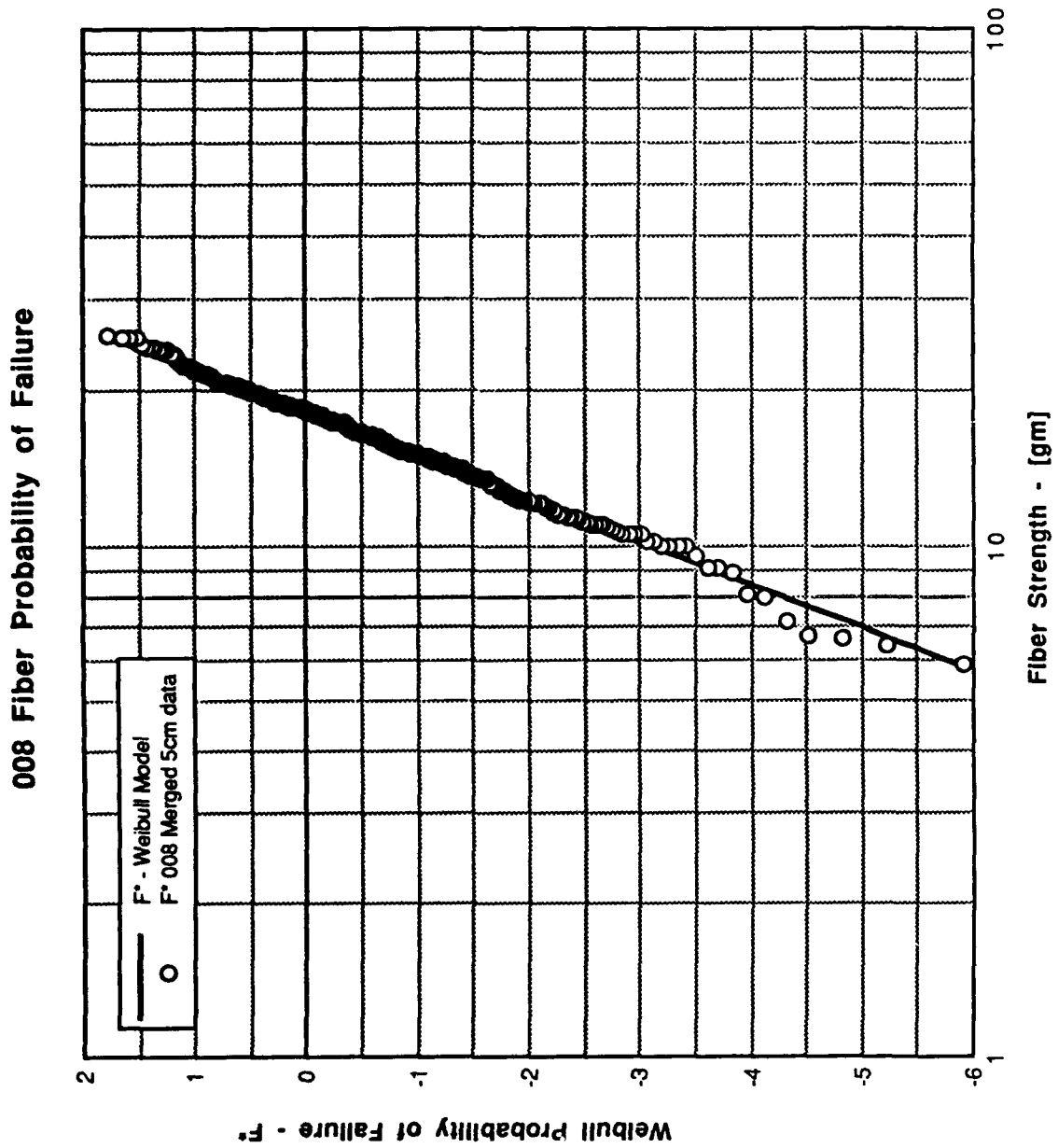


Figure 31. 008 Weibull Model-Merged Fiber Data Comparison

019 Fiber Data - Metric Relationship

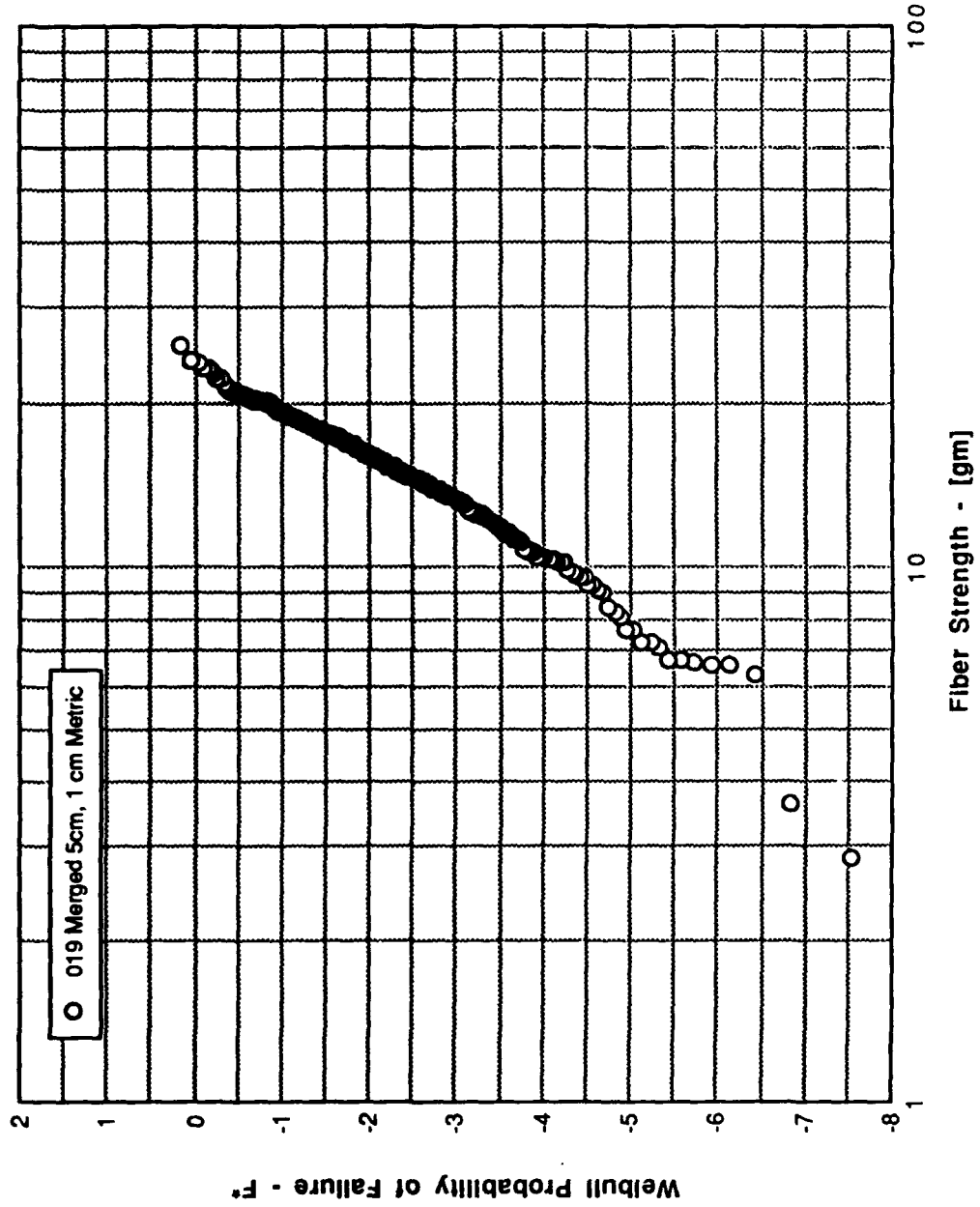


Figure 32. 019 Fiber Data-Metric Relationship

008 Fiber Data - Metric Relationship

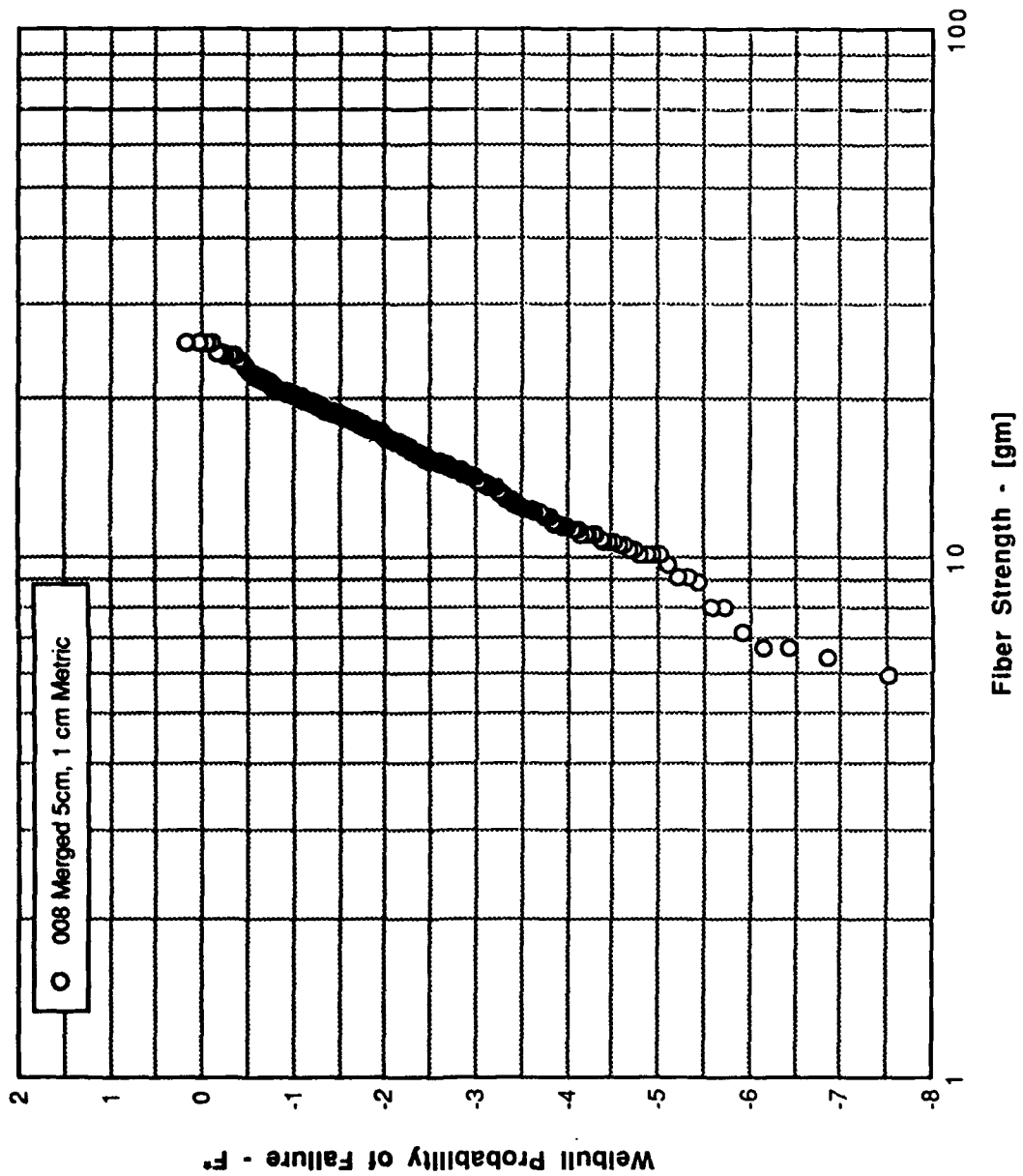


Figure 33. 008 Fiber Data-Metric Relationship

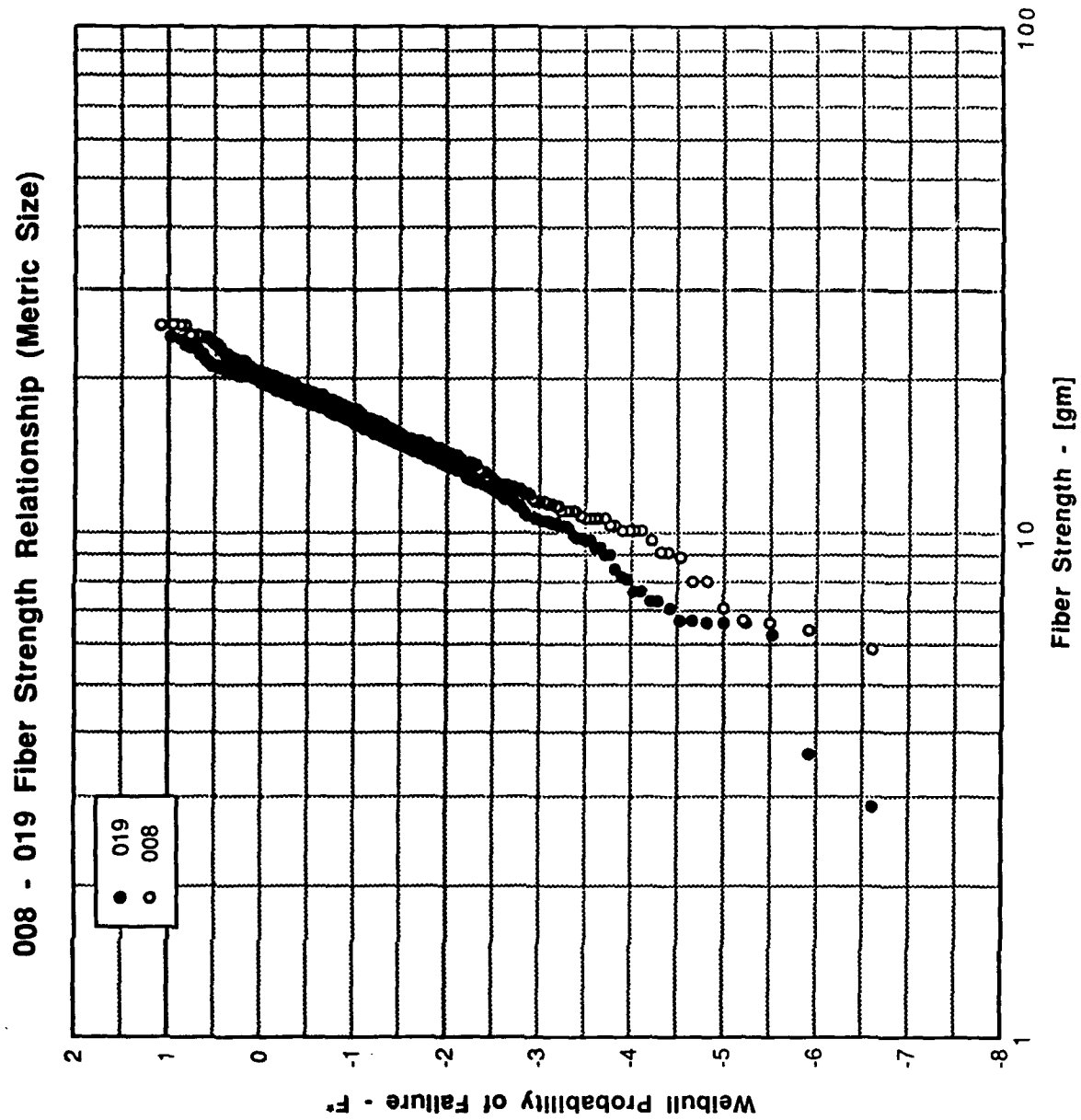


Figure 34. 008-019 Fiber Strength Relationship

019 Fiber/Composite Probability of Failure

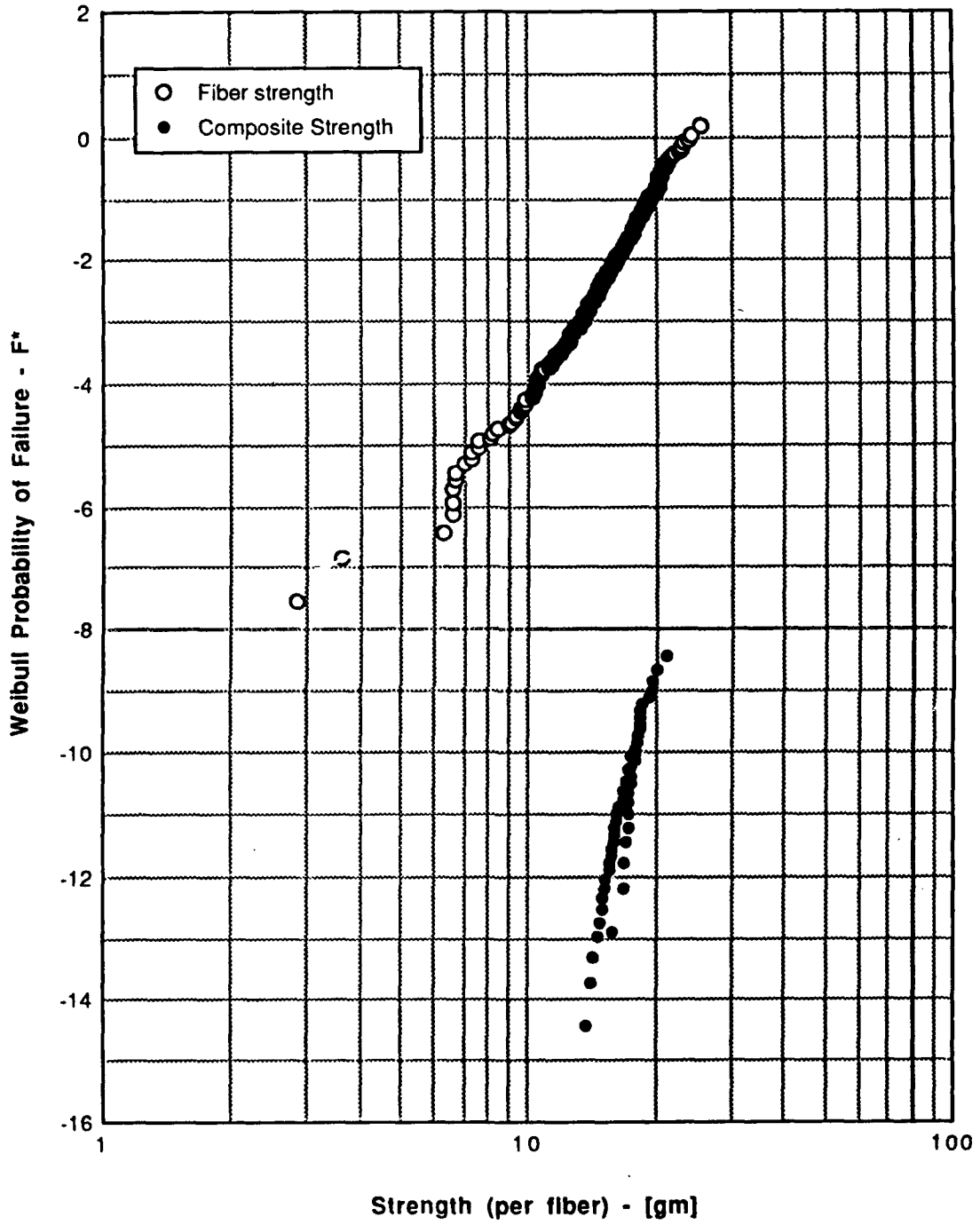


Figure 35. 019 Fiber/Composite Probability of Failure

008 Fiber/Composite Probability of Failure

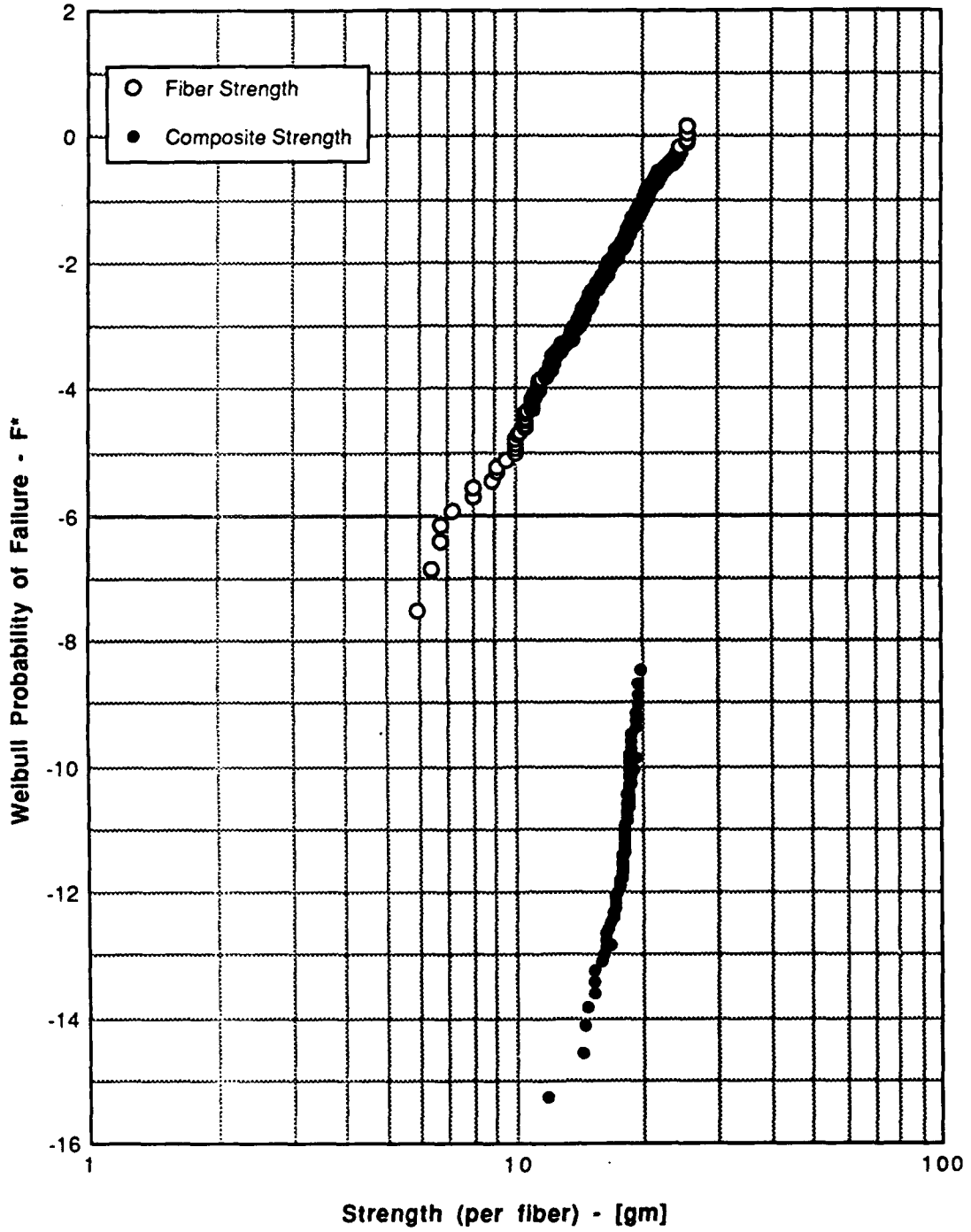


Figure 36. 008 Fiber/Composite Probability of Failure

Relation Between Fiber and Composite Strength Statistics - 008

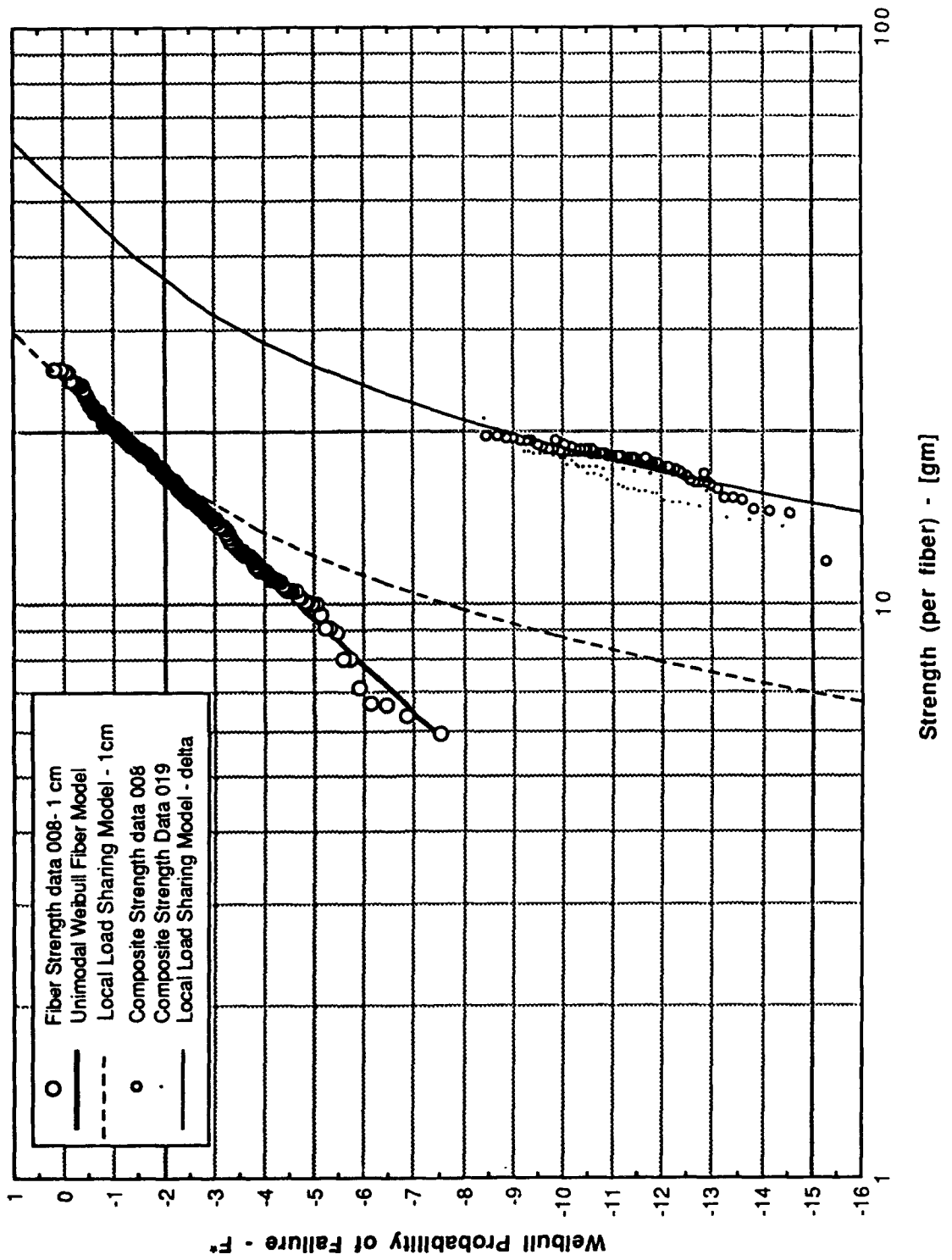


Figure 37. 008 Composite Reliability Prediction Based on Fiber Statistics

Relation Between Fiber and Composite Strength Statistics - 019

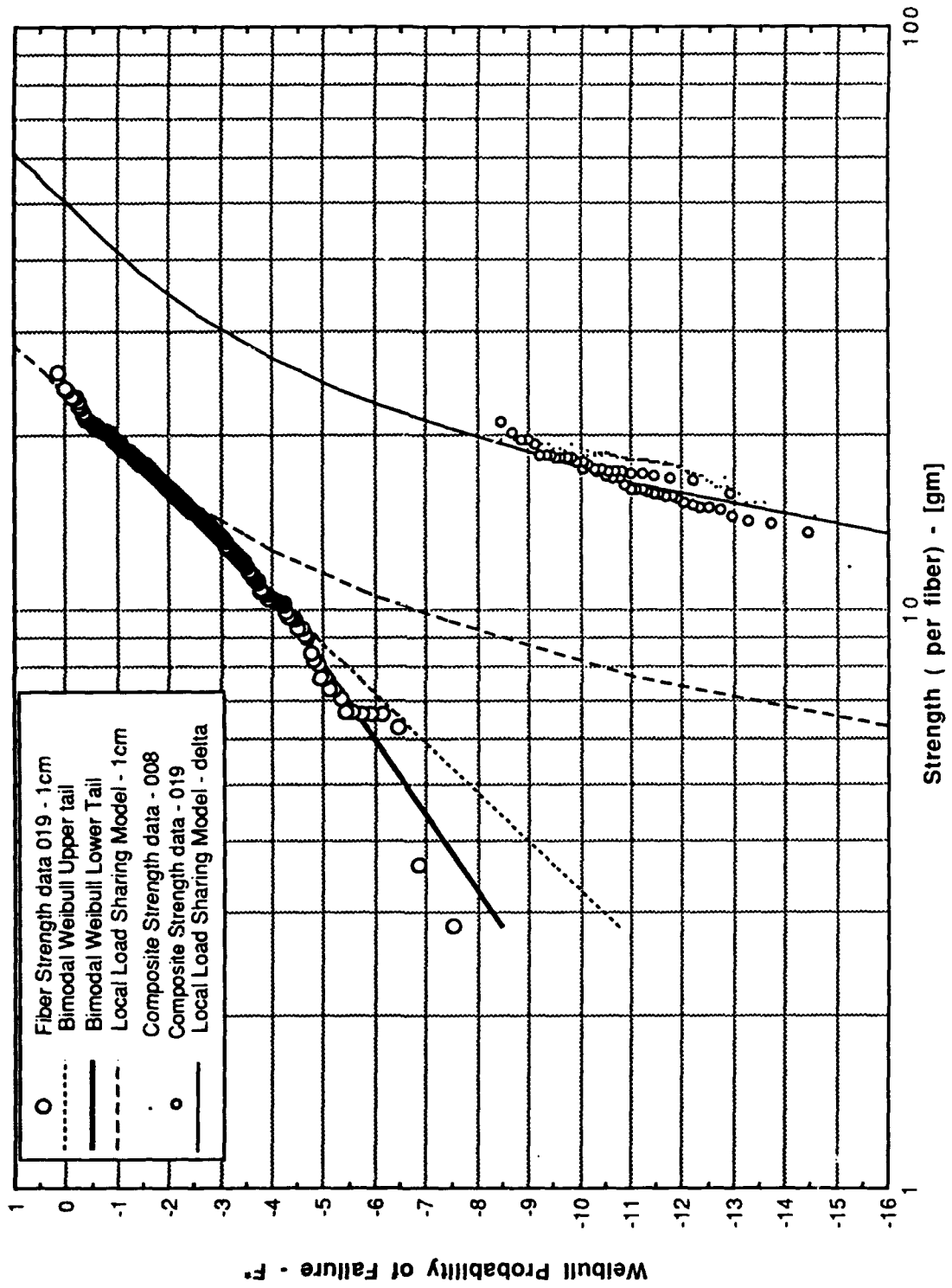


Figure 38. 019 Composite Reliability Prediction Based on Fiber Statistics

APPENDIX B

TABLE I. CALIBRATION DATA

Calibration Load (lbs)	Test Instrument Load (lbs)			Calibration Drift (%)
	Before	During	After	
0	0.059	0.059	0.059	---
11.023	11.067	11.008	11.127	+0.54
22.046	22.076	22.017	22.135	+0.27
33.069	33.084	33.025	33.202	+0.36
44.092	44.092	43.974	44.092	+0.0
55.116	55.101	55.041	55.160	+0.11
66.139	66.109	66.109	66.168	+0.09
77.162	77.117	77.117	77.236	+0.15
88.185	88.185	88.125	88.244	+0.07
99.208	99.193	99.134	99.252	+0.06
110.231	110.200	110.140	110.200	+0.0

TABLE II. AS4-008 2 INCH GAUGE LENGTH LOAD AND DISPLACEMENT FAILURE DATA

FAILURE LOAD (Kg)	EXPERIMENTAL ¹ CERTAINTY	STRAIN AT FAILURE (mm)
50.44	1	.0330
58.52	0	.0374
56.54	1	.0405
51.76	0	.0410
58.79	0	.0362
55.09	0	.0355
53.99	0	.0350
53.88	0	.0351
57.66	0	.0373
55.84	0	.0357
56.48	0	.0385
58.71	1	.0390
57.61	0	.0362
55.25	0	.0359
55.30	1	.0361
58.25	0	.0388
55.17	0	.0358
57.53	0	.0375
54.63	0	.0358

Note 1: '0' - No known experimental artifacts

'1' - Known experimental artifact - intrinsic strength > failure strength

**TABLE II. AS4-008 2 INCH GAUGE LENGTH LOAD
AND DISPLACEMENT FAILURE DATA
(CONT)**

FAILURE LOAD (Kg)	EXPERIMENTAL ¹ CERTAINTY	STRAIN AT FAILURE
56.00	0	.0355
55.01	0	.0352
53.66	1	.0425
54.25	0	.0452
55.28	0	.0367

Note 1: '0' - No known experimental artifacts

'1' - Known experimental artifact - intrinsic strength > failure strength

**TABLE III. AS4-008 10 INCH GAUGE LENGTH LOAD
AND DISPLACEMENT FAILURE DATA (SET B)**

FAILURE LOAD (Kg)	EXPERIMENTAL ¹ CERTAINTY	STRAIN AT FAILURE (mm)
55.89	0	.1710
53.99	0	.1799
53.77	1	.1732
55.68	0	.1856
55.73	0	.1759
54.07	1	.1748
54.98	1	.1779
53.10	1	.1702
55.33	0	.1782
54.58	0	.1770
47.49	1	.1602
56.24	0	.1773
55.60	1	.1788
51.57	1	.1658
53.83	1	.1761
54.17	0	.1776
54.66	1	.1773
35.57	0	.1181
51.87	0	.1645
52.81	0	.1710
55.68	1	.1809
54.44	1	.1753
56.62	0	.1794
54.17	1	.1714
53.50	0	.1717
53.96	1	.1733
53.05	1	.1735
52.56	0	.1688
54.31	1	.1745
53.15	1	.1763

Note 1: '0' - No known experimental artifacts

'1' - Known experimental artifact - intrinsic strength > failure strength

**TABLE IV. AS4-008 16 INCH GAUGE LENGTH LOAD
AND DISPLACEMENT FAILURE DATA**

FAILURE LOAD (KG)	EXPERIMENTAL CERTAINTY ¹	STRAIN AT FAILURE (mm)
53.42	0	.2745

Note 1: '0' - No known experimental artifacts

'1' - Known experimental artifact - intrinsic strength > failure strength

**TABLE V. AS4-008 5 INCH GAUGE LENGTH LOAD
AND DISPLACEMENT FAILURE DATA**

FAILURE LOAD (Kg)	EXPERIMENTAL ¹ CERTAINTY	STRAIN AT FAILURE (mm)
55.52	0	.0896

Note 1: '0' - No known experimental artifacts

'1' - Known experimental artifact - intrinsic strength > failure strength

TABLE VI. AS4-019 2 INCH GAUGE LENGTH LOAD AND DISPLACEMENT FAILURE DATA

FAILURE LOAD (KG)	EXPERIMENTAL CERTAINTY ¹	STRAIN AT FAILURE (mm)
54.50	0	.0365
57.74	0	.0339
58.79	0	.0328
60.24	0	.0333
58.93	0	.0372
54.98	0	.0336
51.60	0	.0341
62.95	1	.0338
47.25	0	.0320
52.08	0	.0344
52.30	0	.0362
53.29	0	.0361
51.57	0	.0361
53.74	0	.0345
55.03	0	.0355
53.91	1	.0347
51.89	0	.0337
54.58	0	.0403
54.79	0	.0384
51.03	0	.0332
55.41	0	.0447

Note 1: '0' - No known experimental artifacts

'1' - Known experimental artifact - intrinsic strength > failure strength

**TABLE VI. AS4-019 2 INCH GAUGE LENGTH LOAD
AND DISPLACEMENT FAILURE DATA
(CONT)**

FAILURE LOAD (KG)	EXPERIMENTAL CERTAINTY ¹	STRAIN AT FAILURE (mm)
51.95	0	.0397
54.76	1	.0448
50.09	1	.0330
51.46	0	.0349
50.58	1	.0339

Note 1: '0' - No known experimental artifacts

'1' - Known experimental artifact - intrinsic strength > failure strength

TABLE VII. AS4-019 10 INCH GAUGE LENGTH LOAD AND DISPLACEMENT FAILURE DATA

INTRINSIC LOAD (Kg)	EXPERIMENTAL ¹ CERTAINTY
44.89	0
42.38	0
44.86	0
47.15	0
42.18	0
50.60	0
51.91	0
49.08	0
48.31	0
43.47	0
47.69	0
45.61	0
46.79	0
50.35	0
47.29	0
48.44	0
47.54	0
45.18	0
50.80	0
44.48	0
52.22	0
46.53	0
40.80	0
48.05	0

Note 1: '0' - No known experimental artifacts

'1' - Known experimental artifact - intrinsic strength > failure strength

TABLE VIII. AS4-008 10 INCH GAUGE LENGTH LOAD AND DISPLACEMENT FAILURE DATA (SET A)

INTRINSIC LOAD (Kg)	EXPERIMENTAL ¹ CERTAINTY
53.19	0
45.85	0
57.52	0
43.24	0
49.40	0
53.66	0
54.03	0
54.28	0
43.71	0
53.51	0
51.73	0
50.67	0
48.65	0
48.62	0
54.70	0
50.00	0
51.34	0
51.05	0
53.32	0
51.47	0
45.82	0
44.04	0
45.63	0
48.25	0
48.74	0

Note 1: '0' - No known experimental artifacts

'1' - Known experimental artifact - intrinsic strength > failure strength

TABLE IX. WEIBULL DISTRIBUTION PARAMETERS

Test Sample	α	β	AL	TLM	AM	BM	TMU	AU ¹
008 Fiber(1cm)	--	--	5.23	3.75	5.23	24.76	32.00	5.23
019 Fiber(1cm)	--	--	3.31	9.62	5.08	23.75	30.00	5.08
008 Strand (2")	33.62	57.07	--	--	--	--	--	--
008 Strand 10" (Set A)	15.22	51.81	--	--	--	--	--	--
008 Strand 10" (Set B)	26.00	56.09	--	--	--	--	--	--
008 Strand (Merged)	15.83	54.53	--	--	--	--	--	--
019 Strand (2")	14.75	56.52	--	--	--	--	--	--
019 Strand (10")	17.48	48.34	--	--	--	--	--	--

Note 1: Strand distribution is presented in a unimodal format.
 Fiber distribution is presented in a trimodal format to
 facilitate data entry into the LLS program. Abbreviations are

A - α	B - β	T - transition point
L - Lower	M - Middle	U - Upper

APPENDIX C

I. COMPLIANCE CALCULATIONS

To obtain the most accurate load versus displacement representation possible, the raw cross head displacement data must be adjusted to take into account the compliance of the mechanical system itself. The displacement recorded (∂) during data collection is a combination of the compliance of the mechanical system (∂') and that of the test strand (∂'') such that

$$\partial = \partial' + \partial'' \quad (1)$$

Knowing

$$\partial' = P/k, \quad (2)$$

where P is the load and k' is the equivalent spring constant of the mechanical system (which is a constant). For the strand itself,

$$\sigma = E\epsilon \quad \text{or} \quad P/A = E \frac{\partial''}{l} \quad \text{or} \quad \partial'' = \frac{Pl}{AE} \quad (3)$$

where A is the cross-sectional area of the strand
 E is Youngs Modulus
 l is the gauge length of the sample

Note that since the test strands are considered identical, $1/AE$ is a constant.

By substituting equations (2) and (3) into (1) for two samples of different gauge lengths, the resulting system spring constant is

$$k' = \left[\frac{l_2 - l_1}{\frac{\partial_1 l_2}{P_1} - \frac{\partial_2 l_1}{P_2}} \right] \quad (4)$$

Since in data interpretation it's desirable to express k' as a function of a load (P), we take the case where the load is the same for each data point, thus $P_1 = P_2 = P$, therefore equation (4) simplifies to

$$k' = \left[\frac{P(l_2 - l_1)}{\partial_1 l_2 - \partial_2 l_1} \right] \quad (5)$$

Knowing

$$\Delta \partial' = \frac{\Delta P}{k'(P)}$$

we can solve for ∂' at any point by integrating, thus resulting in

$$\partial'_i = \int_0^{P_i} \frac{1}{k'(P)} dP$$

By using equation (5), the system spring constant (k') and compliance (δ'), both functions of load, were calculated at each point that a common value of the load occurred during the testing of two separate gauge length samples. Ideally, compliance data should be taken with a constant load control system instead of a constant cross-head rate control system for

direct data reduction. This feedback control configuration is not available for the testing system used in this investigation; as an alternative, the data from two different gauge length samples were manually reduced and common loads identified in order to conduct the analysis. Another approach that could be taken would be to curve fit the test data, establish an equation (displacement as a function of load) for each set of data, and then simply calculate the displacements at the desired loads.

Four samples of varying gauge lengths (2, 5, 10, and 16 inches) were tested and analyzed to obtain the system compliance. The samples were produced as described in the Background section using AS4-008 composite strands. All combinations of $\partial'(P)$ computed from the four samples were compared and the resulting graphical comparison is presented in Figure 1. As shown, system compliance closely correlates in three (2-5 inch, 2-10 inch, and 2-16 inch) of the six combinations. Since the calculated value of $\partial'(P)$ at low loads for the 2-5 inch gauge length compliance is negative, the final compliance calculation excludes this result. Thus, the final system compliance was derived by averaging the 2 and 16 inch gauge length compliance data with the 2 and 10 inch gauge length compliance data which is presented in Figure 2. The equation for the system compliance was obtained by using a third order polynomial curve fit through the averaged data and is

$$\partial'(P) = 9.3062E-5 + 2.8145E-5 P + 7.9643E-8 P^2 + 4.7468E-10 P^3$$

It should be noted that this equation is valid only for loads up to 145 lbs since extrapolation of the curve fit polynomials are not

necessarily valid beyond this point. However, this is sufficient since the maximum loads observed during testing do not exceed this limit.

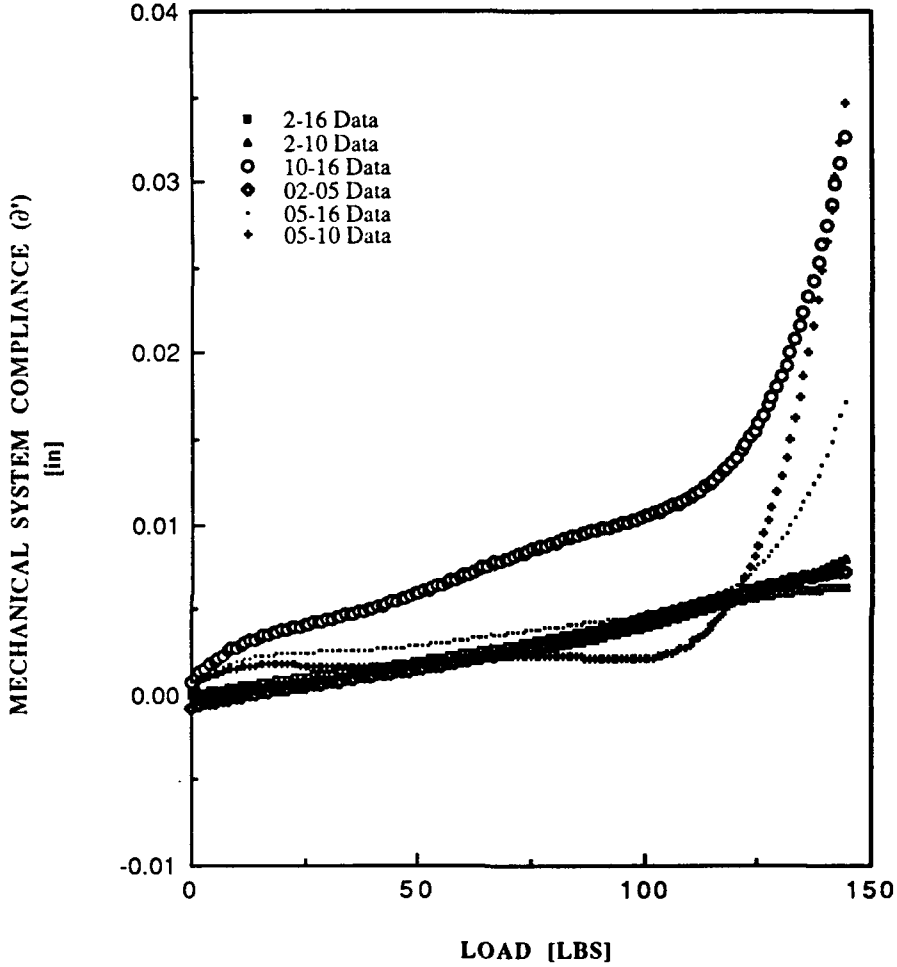


Figure 1. System Compliance Comparison

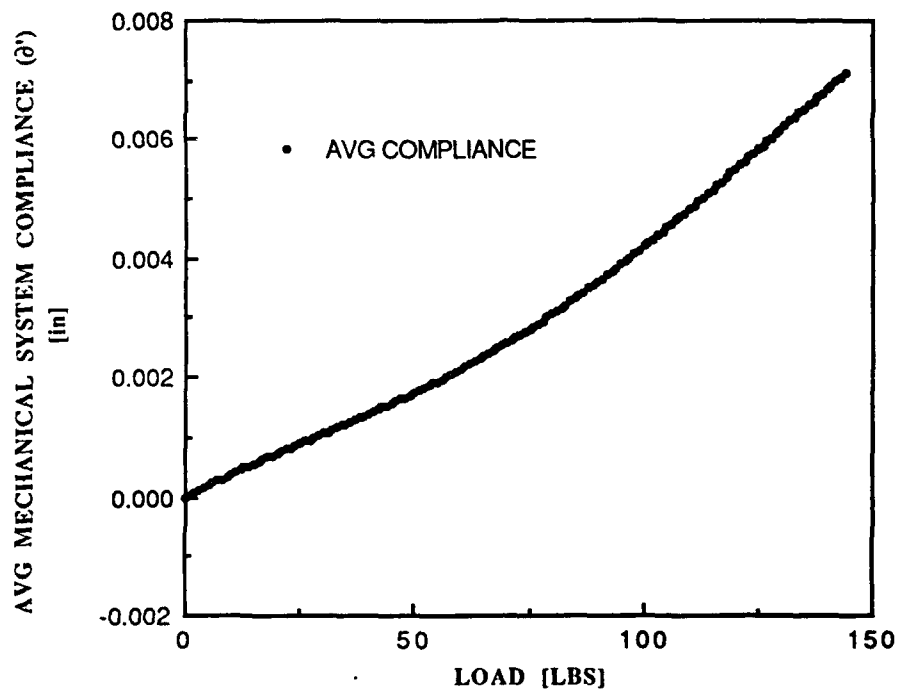


Figure 2. Avg. Mechanical System Compliance

APPENDIX D

I. MERGING OF STRENGTH DATA FROM DIFFERENT SAMPLE DIMENSIONS

There are two different mathematical normalizations of the strength data measured from samples of different dimensions (in the context of this investigation, different gauge lengths). The underlying assumption of the mathematical normalization is that the failure is an extreme value process (weakest link) and that the strength of each segment of the sample (the link) is Independent and Identically distributed.

When data are represented in a transformed Weibull cumulative probability of failure, a horizontal shift of the data can be made which, in effect, shifts the location parameter of the assumed two parameter Weibull distribution model. This results in a shift of the lower tail of the Weibull probability curve down. The derivation for this correction of gauge length is presented in Appendix C of Ref. 7. It should be noted that this method can only be utilized on a two parameter Weibull distributed function (which is linear in the Weibull probability of failure coordinates) or a three parameter function that can be linearized into a two parameter function.

A vertical shift of the data can also be made which maintains the same location parameter but shifts the Weibull probability curve up or down on its vertical scale in order to account for the change in probability associated

with a change in the metric dimension. It can be shown that the reliability of a chain (fiber) is equal to the reliability of a link in the chain (the metric dimension) raised to the power of the number of links in the chain (n), or in terms of probability of failures

$$(1 - F_n(L)) = (1 - F(L))^n$$

where $F_n(L)$ is the probability of failure of the chain and
 $F(L)$ is the probability of failure of a link in the chain

This assumes that the links of the chain are independent and identically distributed. The equation can be written as

$$\ln(1 - F_n(L)) = n \ln(1 - F(L)) \quad \text{or}$$

$$\ln(-\ln(1 - F_n(L))) = \ln n + \ln(-\ln(1 - F(L)))$$

which is observed to be in the form of $x' = c + x$. Therefore, the distribution of the chain preserves any and all distributions of the link and the distribution of the chain is simply a vertical shift of the link by $\ln n$ (the physical size of the chain). Note that the use of $\ln(-\ln(1 - F_n(L)))$ implies a series of weakest links (Type III, extreme value statistics) and if it is linear, then it implies a Weibull distribution. The same procedure used in the above mathematical derivation is also valid for a composite with load sharing. Applying these procedures results in

$$\ln(-\ln(1 - H_{mn}(L))) = \ln(mn) + \ln(-\ln(1 - W(L)))$$

where $H_{mn}(L)$ is the probability of failure of a composite of length l
(given mn) where l is the gauge length

$W(L)$ is the probability of failure of a composite at the
desired metric length

n is the number of fibers in the bundle

m is the number of bundles (segments of the length
of the metric) in the gauge length

Note that this again is in the form of $x' = c + x$ and that the transformation
simply involves a shift in the vertical axis. Rearranging, we have

$$\ln(-\ln(1 - W(L))) = \ln(-\ln(1 - H_{mn}(L))) - \ln(mn)$$

This relation is used to transform strength data measured from different
gauge lengths into one common gauge length. This normalization of all
data into one reference metric dimension allows the merging or pooling of
the aforementioned strength data for comparison with the analytical Local
Load Sharing probability predictions.

APPENDIX E

I. MAXIMUM LIKELIHOOD ESTIMATOR

A. BACKGROUND

The Maximum Likelihood Estimator (MLE) method is a method of estimating the parameters of a model (curve) for a given set of data. There are several advantages of the MLE method over the least squares method. The least squares method assumes equal weighting of the data in the linearized domain and does not account for data clustering. In addition, it can only be used with exact ($x = x_j$) data, where x is the true realization of the data and x_j is the experimental data. The MLE method, on the other hand, correctly weights the data by the probability of occurrence and it is applicable for exact ($x = x_j$), interval ($x_j < x < x_{j+1}$), or censored ($x > x_j$) data. A data set may consist of one or more of the three classes of data. The MLE method is statistically sufficient, asymptotically consistent, asymptotically efficient, and converges to the underlying parameters.

The principle behind the MLE method is to determine the model parameters of the assumed model that has the maximum likelihood, or probability, of repeating a particular set of data from all possible repetitions. In developing the mathematical representation of the MLE method, it is assumed that the combined probability of *all* the data

occurring during testing is the product of the probability of each data point in the set, or

$$\prod_{i=1}^n f(x_i, \theta) = [f(x_1, \theta)][f(x_2, \theta)][f(x_3, \theta)] \dots [f(x_n, \theta)] \quad (1)$$

where $f(x_i, \theta)$ is the probability of one of n data points given the model parameters θ . This assumes that the data were collected from identical, independent samples. The likelihood (L) is therefore defined as this combined probability, or

$$L \equiv \prod_{i=1}^n f(x_i, \theta) \quad (2)$$

One notes that to solve for the likelihood (L), the probability function $f(x_i, \theta)$ must be known, which includes both the data and the model parameters. The problem, of course, is that the parameters are not known.

One approach to solving this problem is to conduct an iterative calculation process such that you assume values of α and β , and solve for (L). The likelihood (L) is then plotted as a function of α and β , resulting in a 3-D plot. Different values for α and β are then chosen and another L is calculated and plotted. This process is continued until the plot can be analyzed and the peak or maximum likelihood determine. These values of α and β become the estimated parameters of the model.

There are several problems associated with this process. First, since $f(x_i, \theta) < 1$, it implies that

$$\prod_{i=1}^n f(x_i, \theta) \ll 1$$

and for large sample sizes, the computer's numerical capacity can be underflowed. In addition, the evaluation of where the maximum likelihood occurs involves the use of a concept dealing with Confidence Regions, which turn out to be coupled with associated Confidence Intervals for the parameters. The evaluation of (L) can then become quite complicated.

Another solution to the problem is to solve directly for α and β . This solution maximizes the likelihood (L) analytically by taking the derivative (with respect to the model parameters) of equation (2) and setting them equal to zero. For the two parameter Weibull distribution, these mathematical steps can be performed explicitly resulting in two equations with the two unknown model parameters (α and β). These two equations are then solved simultaneously for the model parameters. As it turns out, the equations for α and β are decoupled such that one parameter (normally α) can be optimized and then the other parameter (β) calculated.

B. CENSORED DATA WITH KNOWN BUT DIFFERENT LOWER BOUNDS (WEIBULL DISTRIBUTION)

1. Definition of Variables

n \equiv Total number of tests

m \equiv Number of tests of known realized strength (no uncertainty)

x_i \equiv Exact data

\hat{x}_i \equiv Realized data where $\hat{x}_i \leq x_i$ (uncertain data)

θ \equiv Parameters of the assumed model

The likelihood is the product of all the individual probabilities, but the exact value for the uncertain data is unknown. What is known is that the exact data is at least as great as or equal to the uncertain data. Therefore the likelihood is

$$L = \left[\prod_{i=1}^m f(x_i, \theta) \right] \left[\int_{\hat{x}_i}^{\infty} f(x, \theta) dx \right] \left[\int_{\hat{x}_i}^{\infty} f(x, \theta) dx \right] \dots$$

or

$$L = \left[\prod_{i=1}^m f(x_i, \theta) \right] \left[\prod_{i=m}^n \left\{ \int_{\hat{x}_i}^{\infty} f(x, \theta) dx \right\} \right]$$

Knowing that

$$\int_{\hat{x}_i}^{\infty} f(x, \theta) dx = 1 - \int_0^{\hat{x}_i} f(x, \theta) dx = 1 - F(\hat{x}_i, \theta)$$

the likelihood is then

$$L = \left[\prod_{i=1}^m f(x_i, \theta) \right] \left[\prod_{i=m}^n (1 - F(\hat{x}_i, \theta)) \right]$$

For a 2 parameter Weibull distribution we know

$$f(x, \theta) = \frac{\alpha x^{\alpha-1}}{\beta^\alpha} \exp\left\{-\left(\frac{x}{\beta}\right)^\alpha\right\}$$

and

$$1 - F(\hat{x}_i; \theta) = \exp \left\{ - \left(\frac{\hat{x}_i}{\beta} \right)^\alpha \right\}$$

Therefore

$$L = \left[\prod_{i=1}^m \frac{\alpha x_i^{\alpha-1}}{\beta^\alpha} \exp \left\{ - \left(\frac{x_i}{\beta} \right)^\alpha \right\} \right] \left[\prod_{i=m}^n \exp \left\{ - \left(\frac{\hat{x}_i}{\beta} \right)^\alpha \right\} \right]$$

or

$$L = \left[\alpha^m \beta^{-m\alpha} \prod_{i=1}^m \left\{ x_i^{(\alpha-1)} \exp \left\{ - \left(\frac{x_i}{\beta} \right)^\alpha \right\} \right\} \right] \left[\prod_{i=m}^n \exp \left\{ - \left(\frac{\hat{x}_i}{\beta} \right)^\alpha \right\} \right]$$

2. Maximizing L with Respect to α and β

To remove the multiplicative products from the above equation, we take the natural log (ln) of L such that $\ln(L) = L$. Therefore

$$L = m \ln(\alpha) - m\alpha \ln(\beta) + \sum_{i=1}^m (\alpha - 1) \ln(x_i) - \beta^{-\alpha} \sum_{i=1}^m x_i^\alpha + \beta^{-\alpha} \sum_{i=m}^n \hat{x}_i^\alpha$$

To maximize L (equivalent to maximizing $\ln(L)$) with respect to α and β , the partial derivatives are taken and set equal to zero, or

$$\frac{\delta L}{\delta \alpha} = 0 \quad \text{and} \quad \frac{\delta L}{\delta \beta} = 0$$

This results in

$$\frac{\delta L}{\delta \alpha} = 0 = m\alpha^{-1} + \sum_{i=1}^m \ln(x_i) - \ln(\beta) \left(m - \beta^{-\alpha} \left[\sum_{i=1}^m x_i^\alpha + \sum_{i=m}^n \hat{x}_i^\alpha \right] \right) - \beta^{-\alpha} \left[\sum_{i=1}^m (x_i^\alpha \ln(x_i)) \right]$$

$$\beta^{-\alpha} \left[\sum_{i=1}^n \left[\hat{x}_i^{\alpha} \ln(\hat{x}_i) \right] \right] \quad (3)$$

and

$$\frac{\delta L}{\delta \beta} = 0 = -m\alpha + \alpha\beta^{-\alpha} \left(\sum_{i=1}^m x_i^{\alpha} + \sum_{i=m}^n \hat{x}_i^{\alpha} \right)$$

The above equation simplifies to

$$m = \beta^{-\alpha} \left[\sum_{i=1}^m x_i^{\alpha} + \sum_{i=m}^n \hat{x}_i^{\alpha} \right]$$

or

$$\beta = \left\{ m^{-1} \left[\sum_{i=1}^m x_i^{\alpha} + \sum_{i=m}^n \hat{x}_i^{\alpha} \right] \right\}^{\frac{1}{\alpha}} \quad (4)$$

Substituting (4) into (3) and solving for α and β produces

$$\alpha = \left\{ \frac{\frac{1}{m} \sum_{i=1}^m (x_i^{\alpha} \ln(x_i)) + \frac{1}{m} \sum_{i=1}^n (\hat{x}_i^{\alpha} \ln(\hat{x}_i))}{\frac{1}{m} \sum_{i=1}^m x_i^{\alpha} + \frac{1}{m} \sum_{i=m}^n \hat{x}_i^{\alpha}} - \frac{1}{m} \sum_{i=1}^m \ln(x_i)} \right\}^{-1}$$

and

$$\beta = \left\{ \frac{1}{m} \sum_{i=1}^m x_i^{\alpha} + \frac{1}{m} \sum_{i=m}^n \hat{x}_i^{\alpha} \right\}^{\frac{1}{\alpha}}$$

We note that the shape and scale parameters α and β are decoupled but α is implicit. Either an iteration calculation or numerical methods are used to solve for the shape parameter α . Once α is found, β is calculated directly. We further note that the equations for α and β can also be used for non-censored data by simply letting $m = n$.

LIST OF REFERENCES

1. Rosen, B. W., *Tensile Failure of Fibrous Composites*, Journal of American Institute of Aeronautics and Astronautics, vol.2, no. 11, pp. 1985-1991, November 1964.
2. Harlow, D. G. and Phoenix, S.L., *The Chain-of-Bundles Probability Model for the Strength of Fibrous Materials I: Analysis and Conjectures*, Journal of Composite Materials. Vol.12, pp.195-214. 1978
3. Harlow, D. G. and Phoenix, S.L., *The Chain-of-Bundles Probability Model for the Strength of Fibrous Materials II: A Numerical Study of Convergence*, Journal of Composite Materials. Vol.12, pp.314-334. 1978
4. Metcalf, A. G. and Schmitz, G. K., *Effect of Length on the Strength of Glass Fibers*, American Society of Testing Materials, Preprint 87(1964).
5. Phoenix, S. L. and Smith R. L., *A Comparison of Probabilistic Techniques for the Strength of Fibrous Materials Under Local Load-Sharing Among Fibers*, International Journal of Solid Structures, vol.19, no.6, pp. 479-496, 1983.
6. Test data by Edward M. Wu and Glenn Nypiuk, Lawrence Livermore National Laboratory, 1983.
7. Bell, D. K., *Composite Reliability Enhancement via Preloading*, Master's Thesis, Naval Postgraduate School, Monterey, California, June 1987.

8. Englebert, C. R., *Statistical Characterization of Graphite Fiber for Prediction of Composite Structure Reliability*, Master's Thesis, Naval Postgraduate School, Monterey, California, June 1990.
9. Wu, E. M., "Constituent Fiber Strength Analysis," Internal Report, Advanced Composite Laboratory, Naval Postgraduate School, Monterey, California, October 1989.
10. Harlow, D.G. and Wu, E. M., *Chain-of Bundles Probabilty Model for Unidirectional Composites with Trimodal Weibull Parent Fiber*, manuscript in preparation, 1991.

INITIAL DISTRUBUTION LIST

	No. Copies
1. Defense Technical Information Center Cameron Station Alexandria, VA 22304-6145	2
2. Superintendent Attn: Library, Code 52 Naval Post Graduate School Monterey, CA 93942-5000	2
3. Dr. Edward M. Wu Professor of Aeronautics, Code AA/Wu Naval Post Graduate School Monterey, CA 93942-5000	3
4. Dr. M.R. Gorman Professor of Aeronautics, Code AA/Co Naval Post Graduate School Monterey, CA 93942-5000	1
5. Superintendent Attn: Aeronautical Engineering Curricular Office, Code 31 Naval Post Graduate School Monterey, CA 93942-5000	1
6. Superintendent Attn: Aeronautical Engineering Office, Code AA Naval Post Graduate School Monterey, CA 93942-5000	1

7. Dr. Robert Badaliance 1
Naval Research Laboratory, Code 6380
Branch Head/Mechanics of Materials
Washington, D.C. 20375
8. Dr. Joseph M. Augl 1
Naval Surface Warfare Center
White Oaks (Code R31)
Silverspring, MD 20903-5000
9. Dr. S.C. Chou 1
Chief, Material Dynamics Branch
Army Materials Technology Laboratory
Attn: SLCMT-MRD
Watertown, MA 02171-0001
10. Carl R. Engelbert, CDR, USN 1
Harrier DET LONDON
Box 75
FPO New York, NY 09510-1900
11. Eric P. Johnson, LCDR, USN 1
6906 Olsen Rd.
Pensacola, FL 32506